When Do Visual Category Representations Emerge in Infants' Brains?

Xiaoqian Yan[1,2,3*], Sarah Tung[1+], Bella Fascendini[1+], Yulan Diana Chen[1,2], Anthony M. Norcia[1,2#], Kalanit Grill-Spector[1,2,4#]

1. Department of Psychology, Stanford University, Stanford, CA 94305, USA
2. Wu Tsai Neurosciences Institute, Stanford University, Stanford, CA 94305, USA
3. Institute of Science and Technology for Brain-Inspired Intelligence, Fudan University, Shanghai, China
4. Neurosciences Program, Stanford University, Stanford, CA 94305, USA

* corresponding author

\# co-senior-author

\+ equal contribution

Key words: Infant, object categorization, EEG

Abstract

Organizing the continuous stream of visual input into categories like places or faces is important for everyday function and social interactions. However, it is unknown when neural representations of these and other visual categories emerge. Here we used steady state evoked potential electroencephalography to measure cortical responses in infants at 3-4 months, 4-6 months, 6-8 months, and 12-15 months, when they viewed controlled, gray-level images of faces, limbs, corridors, characters, and cars. We found that distinct responses to these categories emerge at different ages. Reliable brain responses to faces emerge first, at 4-6 months, followed by limbs and places around 6-8 months. Between 6-15 months response patterns become more distinct, such that a classifier can decode what an infant is looking at from their brain responses. These findings have important implications for assessing typical and atypical cortical development as they not only suggest that category representations are learned, but also that representations of categories that may have innate substrates emerge at different times during infancy.

Introduction

Visual categorization is important for everyday activities and is amazingly rapid: adults categorize the visual input in about one-tenth of a second[1,2]. In adults and school-age children, this key behavior is supported by both clustered and distributed responses to visual categories in high-level visual cortex in ventral and lateral temporal cortex (VTC and LOTC, respectively)[3,4]. A visual category consists of items that share common visual features and configurations[2,5–8]; e.g., corridors share features of floors, walls, and ceilings, with a typical spatial relationship. Clustered regions in VTC and LOTC[4,9,10] respond more strongly to items of ecologically-relevant categories (faces, bodies, places, words) than other stimuli[5,11–16] and distributed neural responses across VTC and LOTC[4,9,10] are reliable across items of a category but distinct across items of different categories. However, it is unknown when these visual category representations emerge in infants' brains.

Behaviorally, infants can perform some level of visual categorization within the first year of life. Measurements of infants' looking preferences and looking times suggest that visual saliency impacts young infants' viewing patterns[17]: between 4-10 months of age, infants can behaviorally distinguish between faces and objects[17,18] and between different animals like cats and dogs[19,20]. Later on, between 10-19 months, infants behaviorally distinguish broader-level animate versus inanimate categories[17]. Neurally, electroencephalographic (EEG) studies have found stronger responses to images of faces vs. objects or textures in 4-12-month-olds[21–23] and that stimulus category can be decoded from distributed responses slightly but significantly above chance in 6-15-month-olds[24,25]. Functional magnetic resonance imaging (fMRI) studies have found stronger responses to videos of faces[26,27], bodies[27], and places[26,27] vs. objects in clustered regions in VTC and LOTC of 2-10-month-olds. However, because prior studies used different types of stimuli and age ranges, it is unknown when representations to various categories emerge during the first year of life. To address this key open question, we examined when neural representations to different visual categories emerge during infancy using EEG in infants of 4 age groups spanning 3-15 months of age.

We considered two main hypotheses regarding the developmental trajectories of category representations. One possibility is that representations to multiple categories emerge together because infants need to organize the barrage of visual input to understand what they see. Supporting this hypothesis are findings of (i) selective responses to faces, places, and body parts in VTC and LOTC of 2-10-month-olds[27], and (ii) above chance classification of distributed EEG responses to toys, bodies, faces, houses in 6-8 month-olds[25] as well as animals and body parts in 12-15-month-olds[24].

Another possibility is that representations of different categories may emerge at different times during infancy. This may be due to two reasons. First, representations of ecologically-relevant categories like faces, body parts, and places may be innate because of their evolutionary importance[28–31], whereas representations for other categories may develop later only with learning[5,10,32]. Supporting this hypothesis are findings that newborns and young infants tend to orient to faces[33] and face-like stimuli[34], as well as have cortical responses to face-like stimuli[35], but word representations only emerge in childhood with the onset of reading instruction[5,10,36]. Second, even if visual experience is necessary for the development category representations (including faces[37–40]), categories that are seen more frequently earlier in infancy may develop before others. Measurements using head mounted cameras suggest that infants' visual diet (composition of visual input) varies across categories and age: The visual diet of 0-3-month-olds contains ~25% faces and <10% hands, that of 12-15-month-olds contains ~20% faces and ~20% hands[41,42], and that of 24-month-olds contains ~10% faces, and ~25% hands. Thus, looking behavior in infants predicts that representations of faces may emerge before that of limbs.

<insert Fig 1 here>

Results

45 infants from four age groups: 3-4 months (n = 17, 7 females), 4-6 months (n = 14, 7 females), 6-8 months (n = 15, 6 females), and 12-15 months (n = 15, 4 females) participated in EEG experiments. Twelve participants were part of an ongoing longitudinal study and came for several sessions spanning at least 3 months apart. Infants viewed gray-scale images from five visual categories present in infants' environments (faces, limbs, corridors, characters, and cars) while EEG was recorded. Different from prior infant studies[21,23–27], we used images that have been widely used in fMRI studies[5,7,43–45] and are largely controlled for low-level properties such as luminance, contrast, similarity, and spatial frequency (**Fig 1B** and supplementary **Table S3**). We use a Steady-State Visual Evoked Potential[23,46–48] (SSVEP) paradigm: In each 70-s sequence, images from five categories were shown every 0.233-s; one of the categories was the target, so different images from that category appeared every 1.167-s, and the rest of the images were drawn from the other four categories in a random order (**Fig 1A**). Images of all categories appeared at equal probability and no images were repeated[8]. Infants participated in 5 conditions, which varied by the target category. We used the EEG-SSVEP approach because: (i) it affords a high signal-to-noise ratio with short acquisitions making it effective for infants[23,46], (ii) it has been successfully used to study responses to faces in infants[23,46,49], and (iii) it enables measuring both general visual response to

images by examining responses at the image presentation frequency (4.286 Hz), as well as category-selective responses by examining responses at the category frequency (0.857 Hz, **Fig 1A**).

As the EEG-SSVEP paradigm is novel and we are restricted in the amount of data we can obtain in infants, we first tested if we can use this paradigm and a similar amount of data to detect category-selective responses in adults. Results in adults validate the SSVEP paradigm for measuring category-selectivity: as they show that (i) category-selective responses can be reliably measured using EEG-SSVEP with the same amount of data as in infants (Supplementary **Figs S1-S2**), and that (ii) category information from distributed spatiotemporal response patterns can be decoded with the same amount of data as in infants (Supplementary **Fig S3**).

As infants have lower cortical visual acuity, we also tested if the stimuli are distinguishable to infants. Thus, we simulated how they may look to infants by filtering the images to match the cortical acuity of 3-month-olds Supplementary **Fig S4**). Despite being blurry, images of different categories are readily distinguishable by adults (Supplementary **Movies 1-5**), suggesting that there is sufficient visual information in the lower spatial frequencies of the stimuli for infants to distinguish visual categories.

Robust visual responses in occipital regions to visual stimuli in all infant age groups

We first tested if there are significant visual responses to our stimuli in infants' brains by evaluating the amplitude of responses at the image presentation frequency (4.286 Hz) and its first three harmonics. We found that in all age groups, visual responses were concentrated spatially over occipital electrodes (**Fig 2A-D, left panel, Supplementary Figure S1A**). Quantification of the mean visual response amplitude over a region of interest (ROI) spanning 9 electrodes over early visual cortex (occipital ROI) revealed significant responses in all infant age groups at the image frequency and its first 3 harmonics (response amplitudes significantly above zero with FDR corrected at 4 levels; except for the first harmonic at 8.571 Hz in 6-8-month-olds; **Fig 2A-D, right panel**). Analysis of visual responses separately by category condition revealed that visual responses were not significantly different across category conditions (**Supplementary Fig S5;** no significant main effect of category, $\beta_{category} = 0.08$, 95% CI: -0.08 – 0.24, $t_{(301)} = 0.97$, $p = .33$, or category by age interaction, $\beta_{category\ x\ age} = -0.04$, 95% CI: -0.11 – 0.03, $t_{(301)} = -1.09$, $p = .28$, LMM on response amplitude to 4.286 Hz and its first three harmonics). We also tested if experimental noise varied across age groups. Noise level was estimated in the occipital electrodes by measuring the amplitude of response in frequencies up to 8.571 Hz excluding image presentation frequencies (4.286 Hz and harmonics) and category frequencies (0.857 Hz and harmonics) as this frequency range includes the

relevant main harmonics. We found no significant difference in noise across age groups (**Fig 2E**). These analyses indicate that infants were looking at the stimuli as there are significant visual responses even in the youngest 3-4- month-old infants' and there are no significant differences in noise levels across infants of different ages.

<insert Fig 2 here>

Prior EEG data[21,50] suggest that the timing and waveform of visual responses may vary across development. To complement the frequency domain analysis, we transformed the responses at image frequency and its harmonics to the time domain using an inverse Fourier transformation for two reasons. First, the time-domain provides access to information about response timing and waveform that is not directly accessible from an analysis of responses of individual harmonics. Second the total visual response is better reflected in the time-domain as the individual harmonic amplitudes can sum constructively.

We observed that during the 233-ms image presentation, temporal waveforms had two deflections in 3-4-month-olds (one negativity and one positivity, **Fig 2F**) and four deflections for infants older than 4 months (two minima and two maxima, **Fig 2F**). To evaluate developmental effects, we examined the latency and amplitude of the peak visual response during two time-windows related to the first deflection (60-90 ms), and the second deflection (90-160 ms for 3-4-month-olds, and 90-110 ms for other age groups). In general, we find that the latency of the peak deflection decreased from 3 to 15 months (**Fig 2G, H**). As data includes both cross-sectional and longitudinal measurements and we observed larger development earlier than later in infancy, we used a linear mixed model (LMM) to model peak latency as a function of the logarithm of age (see Methods). Results reveal that the latency of the peak deflection significantly and differentially decreased with age in the two time-windows ($\beta_{\text{age x time window}}$ = -45.78, 95% CI: -58.39 – -33.17, $t_{(118)}$ = -7.19, $p = 6.39 \times 10^{-11}$; LMM with age and time window as fixed effects, and participant as a random effect, all stats in **Supplementary Table S4-S5**). There were larger decreases in the peak latency in the second than first time window (**Fig 2G, H**, first: β_{age} = -7.44, 95% CI: -13.82 – -1.06, $t_{(118)}$ = -2.33, $p_{FDR} < .05$; second: β_{age} = -46.91, 95% CI: -56.56 – -37.27, $t_{(59)}$ = -9.73, $p_{FDR} < .001$). Peak amplitude also differentially develops across the two windows ($\beta_{\text{age x time window}}$ = -4.90, 95% CI: -8.66 – -1.14, $t_{(118)}$ = -2.58, p = .01, Supplementary **Table S6-S7**). The decrease in peak amplitude with age was significant only for the second deflection (β_{age} = -3.59, 95% CI: -6.38 – -0.81, $t_{(59)}$ = -2.58, p = .01, LMM). These data suggest that the temporal dynamics of visual responses over occipital cortex develop from 3 to 15 months of age.

What is the nature of category-selective responses in infants?

We next examined if in addition to visual responses to the rapid image stream, there are also category-selective responses in infants, by evaluating the amplitude of responses at the category frequency (0.857 Hz) and its harmonics. This is a selective response as it reflects the relative response to images of category above the general visual response. **Fig 3** shows the spatial distribution and amplitude of the mean category response for faces and its harmonics in each age group. Mean category-selective responses to limbs, cars, corridors, and words are shown in Supplementary **Figs S6-S9**. We analyzed mean responses over two ROIs spanning 7 electrodes each over the left and right occipitotemporal cortex where high-level visual regions are located[51].

<insert Fig 3 here>

We found significant group-level category responses to some but not all categories and a differential development of category-selective responses during infancy. The largest and earliest developing category-selective responses were to faces. In contrast to visual responses, which were centered over occipital electrodes (**Fig 2A-D,** left panel), significant categorical responses to faces (at 0.857 Hz and its first harmonic, 1.714 Hz) were observed over lateral occipitotemporal electrodes (**Fig 3A-D,** left panel). Notably, there were significant responses to faces over bilateral occipitotemporal electrodes in 4-6-month-olds at 0.857 Hz (**Fig 3B,** response amplitudes significantly above zero with Hotelling's T2 statistic, $p_{FDR} < .05$, FDR corrected over 2 levels: the category frequency and its first harmonic), as well as 6-8-month-olds and 12-15-month-olds at the category frequency and its first harmonic (**Fig 3C,D,** both $p_{FDR} < .05$). However, there were no significant responses to faces in 3-4-month-olds at either the category frequency or its harmonics (**Fig 3A, right panel**). These data suggest that face-selective responses start to reliably emerge over lateral occipitotemporal cortex between 4 and 6 months of age.

We did not find significant group-level category-selective responses that survived FDR correction to any of the other categories before 6 months of age (Supplementary **Fig S6-S9,** except for a weak but statistically significant response for cars in the right occipitotemporal ROI in 3-4-month-olds). Instead, we found significant category-selective responses that survived FDR correction for (i) limbs in 6-8-month-olds in the right occipitotemporal ROI (Supplementary **Fig S6**), (ii) corridors in 6-8-month-olds and 12-15 months-old in the left occipitotemporal ROI (Supplementary **Fig S7**), and (iii) characters in 6-8-

188 month-olds in the right occipitotemporal ROI, and in 12-15-month-olds in bilateral occipitotemporal ROI
189 (Supplementary **Fig S8**).

190 We next examined the development of the category-selective responses separately for the right and
191 left lateral occipitotemporal ROIs. The response amplitude was quantified by the root mean square
192 (RMS) amplitude value of the responses at the category frequency (0.857 Hz) and its first harmonic
193 (1.714 Hz) for each category condition and infant. With a LMM analysis, we found significant
194 development of response amplitudes in the both occipitotemporal ROIs which varied by category (left
195 occipitotemporal ROIs: βcategory x age = -0.21, 95% CI: -0.39 – -0.04, $t_{(301)}$ = -2.40, p_{FDR} < .05; right
196 occipitotemporal ROIs: βcategory x age = -0.26, 95% CI: -0.48 – -0.03, $t_{(301)}$ = -2.26, p_{FDR} < .05, LMM as a
197 function of log (age) and category; participant: random effect).

198 We evaluated the temporal dynamics of category-selective waveforms by transforming the data at
199 the category frequency and its harmonics to the time domain. This analysis was done separately for
200 each of the left and right occipitotemporal ROIs for each category and age group. Consistent with
201 frequency domain analyses, average temporal waveforms over lateral-occipital ROIs show significant
202 responses to faces that emerge at ~4 months of age (**Fig 4A,** significant responses relative to zero,
203 cluster-based nonparametric permutation 10,000 times, two-tailed t-test, at p < .05). The temporal
204 waveforms of responses to faces in infants show an initial positive deflection peaking ~500 ms after
205 stimulus onset followed by a negative deflection peaking at ~900 ms. Notably, mean waveforms
206 associated with limbs, corridors, and characters in lateral occipital-ROIs, are different from faces: there
207 is only a single negative deflection that peaks at ~500 ms after stimulus onset, which is significant only in
208 6-8 and 12-15-month-olds (**Fig 4B-D**). There was no significant category response to cars in infants
209 except for a late (~1000 ms) positive response in 4-6-month-olds (**Fig 4E**). These results show that both
210 the timing and waveform differ across categories, which suggests that there might be additional
211 category information in the distributed spatiotemporal response.

212 **<insert Fig 4 here>**

213

214 We next examined the development of the peak response and latency of the category waveforms
215 separately for the right and left lateral occipitotemporal ROIs. We found significant development of the
216 peak response in the right lateral occipitotemporal ROI which varied by category ($\beta_{\text{category x age}}$ = -1.09, 95%
217 CI: -2.00 – -0.14, $t_{(301)}$ = -2.26, p_{FDR} < .05, LMM as a function of log (age) and category; participant:
218 random effect). Post-hoc analyses revealed that the peak response for faces significantly increased from
219 3 to 15 months (**Fig 4A-right,** β_{age} = 7.27, 95% CI: 4.03 – 10.51, $t_{(59)}$ = 4.50, p_{FDR} < .05, LMM as a function

of log(age); participant: random effect) and the peak response for limbs significantly decreased (**Fig 4B-right,** β_{age} = -2.90, 95% CI: -5.41 – -0.38, $t_{(59)}$ = -2.31, p = .02, not significant after FDR correction over 5 category levels). There were no other significant developments of peak amplitude (Supplementary **Tables S8-S9**).

Additionally, for all categories, the latency of the peak response in the right occipitotemporal ROI significantly decreased from 3 to 15 months of age (β_{age} = -173.17, 95% CI: -284.73 – -61.61, $t_{(301)}$ = -3.05, p = .002, LMM as a function of log(age) and category; participant: random effect). We found no significant development of peak latency in the left occipitotemporal ROI (Supplementary **Tables S8-9**).

Are spatiotemporal patterns of responses to visual categories consistent across infants?

As we observed different mean waveforms over the lateral occipital ROIs for the five categories (**Fig 4**), we asked whether the distributed spatiotemporal patterns of brain responses evoked by each category are unique and reliable across infants. We reasoned that if different categories generated consistent distributed spatiotemporal responses, an independent classifier would be able to predict the category an infant was viewing from their distributed spatiotemporal pattern of response. Thus, we used a leave-one-out-cross-validation (LOOCV) approach (**Fig 5A**) and tested if a classifier can decode the category a left-out infant viewed based on the similarity of their distributed spatiotemporal response to the mean response to each of the categories in the remaining N-1 infants. We calculated for each infant the mean category-waveform (same as **Fig 4**) across the occipital and lateral occipitotemporal ROIs and concatenated the waveforms across the three ROIs to generate the distributed spatiotemporal response to a category (**Fig 5A**). The classifier was trained and tested separately for each age group.

Results reveal two main findings. First, the LOOCV classifier decoded category information from brain responses significantly above the 20% chance level in infants aged 6 months and older but not in younger infants (**Fig 5B**, 6-8-month-olds, significant above chance: $t_{(14)}$ = 4.1, p_{FDR} < .01, one-tailed, FDR corrected over 4 age groups; 12-15-month-olds, $t_{(14)}$ = 3.4, p_{FDR} < .01). This suggests that spatiotemporal patterns of responses to different categories become reliable across infants after 6 months of age. Second, examination of classification by category, shows that the LOOCV classifier successfully determined from spatiotemporal responses when infants were viewing faces in 64% of 4-6-month-olds, in 93% of 6-8-month-olds, and 87% of 12-15-month-olds (**Fig 5C**). In contrast, classification performance was numerically lower for the other categories (successful classification in less than 40% of the infants).

This suggests that a reliable spatiotemporal response to faces that is consistent across infants develops after 4 months of age and dominates classification performance.

<insert Fig 5 here>

What is the nature of categorical spatiotemporal patterns in individual infants?

While the prior analyses leverage the power of averaging across electrodes and infants, this averaging does not provide insight to fine-grained neural representations within individual infants. To examine the finer-grain representation of category information within each infant's brain, we examined the distributed spatiotemporal responses to each category across the 23 electrodes spanning the left and right occipitotemporal cortex in each infant. We tested: (i) if categorical representations in an infant's brain are reliable across different images of a category, and (ii) if category representations become more distinct during the first year of life. We predicted that if representations become more similar across items of a category and more dissimilar between items of different categories then category distinctiveness (defined as the difference between mean within and between category similarity) would increase from 3 to 15 months of age.

To examine the representational structure, we calculated representation similarity matrices (RSMs) across odd/even split-halves of the data in each infant. Each cell in the RSM quantifies the similarity between two spatiotemporal patterns: On-diagonal cells of the RSM quantify the similarity of distributed spatiotemporal responses to different images from the same category and off-diagonal cells quantify the similarity of spatiotemporal responses to images from different categories. Categorical structure will manifest in RSMs as positive on diagonal values indicating reliable within-category spatiotemporal responses which are higher than off-diagonal between category similarity (**Fig 6**, Supplementary **Fig S3B** and **Fig S10**).

Examination of mean RSMs in each age group reveals no reliable category information in individuals at 3-4-month-olds or 4-6-month-olds, as within-category similarity is not significantly above zero (**Fig 6A**, 3-4-month-olds: on-diagonal, -0.03 $\pm$ 0.06, p = .96, one-tailed; 4-6-month-olds: on diagonal: 0.009 $\pm$ 0.11, p = .38). However, starting around 6 months some category structure emerges in the RSMs. In particular, distributed responses to faces become reliable as within category similarity for faces is significantly above zero in 6-8-month-olds (**Fig 6A,** 0.31 $\pm$ 0.24, $t_{(14)}$ = 5.1, p_{FDR} < .05, FDR corrected over 5 category levels), and stays reliable in 12-15-month-olds (**Fig 6A,** 0.26 $\pm$ 0.24, $t_{(14)}$ = 4.18, p_{FDR} < .05). Distributed responses to limbs become reliable later on as within category similarity for limbs is

282 significantly above zero in 12-15-months-olds (**Fig 6A,** 0.11 $\pm$ 0.21, $t_{(14)}$ = 1.98, p = 0.03, but not surviving
283 FDR correction at 5 levels).

284 **<insert Fig 6 here>**

285

286 Next, we evaluated the development of category distinctiveness, which was calculated for each
287 category and infant. Individual infants' category distinctiveness is shown in **Fig 6B** (infants ordered by
288 age) and in the scatterplots in **Fig 6C**. In infants younger than 4 months (120 days) category
289 distinctiveness is largely close to zero or even negative, suggesting no differences between
290 spatiotemporal responses to one category vs another. Category distinctiveness increases with age and
291 becomes more positive from 84 to 445 days of age (**Fig 6B,C**). The biggest increase is for faces where
292 after ~6 months of age (194 days) face distinctiveness is consistently positive in individual infants (13/15
293 infants aged 194-364 days and 12/15 infants aged 365-445 days). The increase in distinctiveness is more
294 modest for other categories and appears later in development. For example, positive distinctiveness for
295 limbs and cars in individual infants is consistently observed after 12 months of age (**Fig 6B,C**; limbs: 9/15
296 infants aged 365-445 days vs 5/15 infants aged 194-364 days; cars: 12/15 365-445 days vs 7/15 194-364
297 days).

298 Using LMMs we determined if distinctiveness significantly changed with age (log transformed) and
299 category (participant, random factor). Results indicate that category distinctiveness significantly
300 increased from 3 to 15 months of age (β_{age} = 0.77, 95% CI: 0.54 –1.00, $t_{(301)}$ = 6.62, p = 1.67×10^{-10}), and
301 further that development significantly varies across categories ($\beta_{\text{age x category}}$ = -0.13, 95% CI: -0.2 – -0.06,
302 $t_{(301)}$ = -3.61, p = 3.5×10^{-4}; main effect of category, β_{category} = 0.27, 95% CI: 0.11 – 0.43, $t_{(301)}$ = 3.38, p =
303 8.2×10^{-4}). Post-hoc analyses for each category (**Fig 6C**) reveal that distinctiveness significantly increased
304 with age for faces (β_{age} = 0.9, 95% CI: 0.6 – 1.1, $t_{(59)}$ = 6.8, p_{FDR} < .001), limbs (β_{age} = 0.4, 95% CI: 0.2 – 0.6,
305 $t_{(59)}$ = 5.0, p_{FDR} < .001), characters (β_{age} = 0.2, 95% CI: 0.02 – 0.3, $t_{(59)}$ = 2.2, p_{FDR} < .05), and cars (β_{age} = 0.4,
306 95% CI: 0.2 – 0.5, $t_{(59)}$ = 3.7, p_{FDR} < .001). Post-hoc t-tests show that for faces, the category distinctiveness
307 is significantly above zero after 6 months of age (6-8-month-olds, $t_{(14)}$ = 6.73, p_{FDR} < .05; 12-15-month-
308 olds, $t_{(14)}$ = 5.30, p_{FDR} < .05) and for limbs and cars at 12-15 months of age (limbs: $t_{(14)}$ = 2.19, p_{FDR} < .05;
309 cars: $t_{(14)}$ = 4.53, p_{FDR} < .05). This suggests that category distinctiveness slowly emerges in the visual
310 cortex of infants from 3 to 15 months of age, with the largest and fastest development for faces.

311

312 **Discussion**

We find that both selective responses to items of a category over others across lateral occipital ROIs and the distinctiveness of distributed visual category representations progressively develop from 3 to 15 months of age. Notably, we find a differential development of category-selective responses (**Fig 7**), whereby responses to faces emerge the earliest, at 4-6 months of age and continue to develop through the first year of life. Category-selective responses to limbs, corridors, and characters follow, emerging at 6-8 months of age. Our analysis of the distinctiveness of the distributed spatiotemporal patterns to each category also finds that distributed representations to faces become more robust in 6-8-month-olds and remain robust in 12-15-month-olds. While the distinctiveness of distributed patterns to limbs and cars only become reliable at 12-15 months of age. Together these data suggest a rethinking of the development of category representations during infancy as they not only suggest that category representations are learned, but also that representations of categories that may have innate substrates such as faces, bodies, and places emerge at different times during infancy.

<insert Fig 7 here>

Reliable category representations start to emerge at 4 months of age

While 3-4 months old infants have significant and reliable evoked visual responses over early visual cortex, we find no reliable category representations of faces, limbs, corridors, or characters in these young infants. Both analyses of average responses across lateral occipital ROIs and analyses of distributed spatiotemporal responses across visual cortex find no reliable category representations in 3-4-month-olds, either when examining mean response across an ROI or in distributed spatiotemporal patterns across visual cortex. The earliest categorical responses we find are for faces, and they emerge at 4-6 months of age.

Is it possible that there are some category representations in 3-4-month-olds, but we lack the sensitivity to measure them? We believe this is unlikely, because (i) we can measure significant visual responses from the same 3-4-month-olds, (ii) with the same amount of data, we can measure category selective responses and decode category information from distributed spatiotemporal responses in infants older than 4 months and in adults. As using SSVEP to study high-level representations is a nascent field[52–54], future work can further examine how SSVEP parameters such as stimulus and target category presentation rate may affect the sensitivity of measurements in infants (see review by[54]).

Our findings together with a recent fMRI study in 2-10-month-olds[27] provide accumulating evidence for multiple visual categories representations in infants' brains before the age of one. However, there

are also differences across studies. The earliest we could find reliable group-level category-selective responses for faces was 4-6-month-olds and for limbs and corridors only after 6 months of age. In contrast, Kosakowski and colleagues[27] report category-selective responses to faces, bodies, and scenes in example 4-5-month-olds. Group average data in their study found significant face- and place-selective responses in infants' ventral temporal cortex (VTC) but not in lateral occipital cortex (LOTC), and significant body-selective responses in LOTC, but not VTC. Because Kosakowski et al.[27] report group-averaged data across infants spanning 8 months, their study does not provide insights to the time course of this development. We note that, the studies differ in several ways: (i) measurement modalities (fMRI in [27] and EEG here), (ii) the types of stimuli infants viewed: in [27] infants viewed isolated, colored and moving stimuli, but in our study, infants viewed still, gray-level images on phase-scrambled backgrounds, which were controlled for several low level properties, and (iii) contrasts used to detect category-selective responses, whereby in [27] the researchers identified within predefined parcels – the top 5% of voxels that responded to the category of interest vs. objects, here we contrasted the category of interest vs. all other categories the infant viewed. Thus, future research is necessary to determine whether differences between findings are due to differences in measurement modalities, stimulus format, and data analysis choices.

Face representations emerge around 4-6 months of age

Recognizing faces (e.g., a caregiver's face) is crucial for infants' daily lives. Converging evidence from many studies suggest that infants have significant and reliable face-selective neural responses at 4-6 months of age[22,23,26,55,56]. While some studies report responses to face-like (high contrast paddle-like) stimuli in newborns[34,35,57] and significant visual evoked responses to faces in 3-month-olds[58,59,54,60], these studies have largely compared responses to an isolated face vs. another isolated object. In contrast, we do not find reliable face-selective responses (**Fig 3 & 4**) or reliable distributed representations (**Fig 5 & 6**) to faces in 3-4-month-olds when responses to faces are contrasted to many other items and when stimuli are shown on a background rather than in isolation. Our findings are consistent with longitudinal research in macaques showing that robust cortical selectivity to faces takes several months to emerge[39] and support the hypothesis that experience with faces is necessary for the development of cortical face selectivity[37,39,40].

Our data also reveal that face-selective responses and distributed representations to faces become more robust in 6-8-month-olds and remain robust in 12-15-month-olds. For example, successful decoding of faces in the group level was observed in 80% of individual infants based on several minutes

of EEG data. Reliable distributed spatiotemporal responses to different images of faces become significantly different from responses to images from different categories. This robust decoding has important clinical ramifications as it may serve as an early biomarker for cortical face processing, which is important for early detection of social and cognitive developmental disorders such as Autism[61,62] and Williams Syndrome[63]. Future research is necessary for elucidating the relationship between the development of brain responses to faces to infant behavior. For example, it is interesting that at 6 months of age, when we find robust face representations, infants also start to exhibit recognition of familiar faces (like parents) and stranger anxiety[64].

One fascinating aspect of the development of cortical face selectivity is that among the categories we tested, selectivity to faces seems to emerge the earliest at around 4 months of age, yet the development of selectivity and distributed representations to faces is protracted compared to objects and places[14,65,15]. Indeed, in both our data and prior work, face-selective responses and distributed representations to faces in infants are immature compared to adults[21,25], and a large body of work has shown that face selectivity[5,14,15,50,65–67] and distributed representations to faces[10] continue to develop during childhood and adolescence. This suggests that not only experience during infancy but also life-long experience with faces, sculpts cortical face selectivity. We speculate that the extended cortical plasticity for faces may be due to both the expansion of social circles (family, friends and acquaintances) across the lifespans and also the changing statistics of faces we socialize with (e.g., child and adult faces have different appearance).

A new insight about cortical development: different category representations emerge at different times during infancy

To our knowledge, our study is the first to examine the development of both ROI level and spatiotemporal distributed responses in infants across the first year of life. We note that both analyses find that category information to faces develops before other categories. However, there are also some differences across analyses (**Fig 7**). For example, for limbs and corridors we find significant category-selective responses at the ROI level in lateral occipitotemporal ROIs starting at 6-8 months but no reliable distinct distributed responses across visual cortex at this age. In contrast, for cars, we find an opposite pattern where there is a distinct spatiotemporal pattern in 12-15-month-olds even as there is no significant car-selective response in the ROI level. As these approaches have different sensitivities, they reveal insights to the nature of the underlying representations. For example, as visible in **Fig 4**, limbs and corridor have a clear category selective waveform in both in 6-8 and 12-15-months-olds, but

409 the waveform of limbs and its spatial distribution is not that different from that to corridors, which may
410 explain why distinctiveness of spatiotemporal patterns for limbs is low in 6-8-month-olds (**Fig 6**).
411 Likewise, even as there is no significant response for cars (**Fig 4e**), its spatiotemporal pattern is
412 consistently different than for other categories giving rise to a distinctive spatiotemporal response by 12
413 months (**Fig 6**).

414 In sum, the key finding from our study is that the development of category selectivity during infancy
415 is non-uniform: face-selective responses and representations of distributed patterns develop before
416 representations to limbs and other categories. We hypothesize that this differential development of
417 visual category representations may be due to differential visual experience with these categories
418 during infancy. This hypothesis is consistent with behavioral research using head-mounted cameras that
419 revealed that the visual input during early infancy is dense with faces, while hands become more
420 prevalent in the visual input later in development and especially when in contact with objects[41,42].
421 Additionally, a large body of research has suggested that young infants preferentially look at faces and
422 face-like stimuli[17,18,33,34], as well as look longer at faces than other objects[41], indicating that not only the
423 prevalence of faces in babies' environments but also longer looking times may drive the early
424 development of face representations. Further supporting the role of visual experience in the formation
425 of category selectivity is a study that found that infant macaques that are reared without seeing faces do
426 not develop face-selectivity but develop selectivity to other categories in their environment like body
427 parts[40]. An alternative hypothesis is that differential development of category representations is of
428 maturational origin. For example, we found differences in the temporal dynamics of visual responses
429 among four infant age groups, which suggests that the infant's visual system is still developing during
430 the first year of life. While underlying maturational mechanisms are yet unknown they may include
431 myelination and cortical tissue maturation[68–73]. Future studies can test experience-driven vs.
432 maturational alternatives by examining infants' visual diet, looking behavior, and anatomical brain
433 development and examine responses using additional behaviorally relevant categories such as food[74–76].
434 These measurements can test how environmental and individual differences in visual experiences may
435 impact infants' developmental trajectories. Specifically, a visual experience account predicts that
436 differences in visual experience would translate into differences in brain development, but a
437 maturational account predicts that visual experience will have no impact on the development of
438 category representations.

439 Together our findings not only suggest that visual experience is necessary for the development of
440 visual category representations, including faces, but also necessitate a rethinking of how visual category

representations develop in infancy. Moreover, this differential development during infancy is evident even for categories that have evolutionary importance and may have innate substrates such as faces, bodies, and places[28–31]. Finally, our findings have important ramifications for theoretical and computational models of visual development as well as for the assessment of atypical infant development.

Methods

Participants

Ethical permission for the study was obtained from the Institutional Review Board of Stanford University. Parents of the infant participants provided written informed consent prior to their first visit and also prior to each session if they came for multiple sessions. Participants were paid 20$/hour for participation. Participants were recruited via ads on social media (Facebook and Instagram).

Sixty-two full-term, typically developing infants were recruited. Twelve participants were part of an ongoing longitudinal study that obtained both anatomical MRI and EEG data in infants. Some of the infants participated in both studies and some only in one of the studies. Infants were recruited at around newborn, 3 months, 6 months, and 12 months. We did not recruit infants between 8-12 months of age because around 9 months there is little contrast between gray and white matter in anatomical MRI scans that were necessary for the MRI study. Infants came for several sessions spanning ~3 months apart (seven 3-4-month-olds, three 4-6-month-olds, eight 6-8-month-olds, and twelve 12-15-month-olds). Data from nineteen infants (nine 3-4-month-olds, six 4-6-month-olds, and eight 6-8-month-olds; among whom seven were longitudinal) were acquired in two visits within a two-week span to obtain a sufficient number of valid data epochs. Supplementary **Table S1** contains participants' demographic information (sex and race). The youngest infants were 3 months old, as the EEG setup requires the infants to be able to hold their head and look at the screen in front of them. 23 adults (14 females) also participated in the study. All participants had normal/corrected-to-normal vision and provided written informed consent.

Data e*xclusion criteria:* We excluded participants who had less than 20 valid epochs (1.1667-s/epoch) per category, had noise/muscular artifacts during the EEG recordings, couldn't record data, or had no visual responses over the occipital electrodes. As such, we excluded (1) five infants due to an insufficient number of epochs, (2) two infants who had no visual responses, (3) ten infants due to technical issues during data collection, and (4) three adults due to excessive noise/muscular artifacts during EEG. In total,

472 we report data from 45 infants (Supplementary **Table S1**) and 20 adults (13 females, 19-38 years) that
473 met inclusion criteria.

474 **Visual stimuli**

475 Natural grayscale images of adult faces, limbs, corridors, characters, and cars are used as stimuli,
476 with 144 images per category from the fLOC image database (https://github.com/VPNL/fLoc)[8]. The size,
477 view, and retinal position of the items varied, and the items were overlaid on phase-scrambled
478 backgrounds that were generated from a randomly drawn image in the stimulus set. The images were
479 also controlled for multiple low-level differences between stimuli of different categories including their
480 luminance, contrast, similarity and spatial frequency power distributions using the SHINE toolbox[77]. As
481 only five of ten categories from [8] were used, we evaluated the stimuli used in our experiments to test if
482 they differed in (i) contrast, (ii) luminance, (iii) similarity, and (iv) spatial frequency. Results show that
483 categories were largely matched on most metrics (**Fig 1B** and Supplementary Materials). The stimuli
484 were presented on a gamma-corrected OLED monitor screen (SONY PVM-2451; SONY Corporation,
485 Tokyo Japan) at a screen resolution of 1920 × 1080 pixels and a monitor refresh rate of 60 Hz. When
486 viewed from 70 cm away, each image extended a visual angle of approximately 12°.

487 **EEG Protocol**

488 The experiments were conducted in a calm, dimly illuminated lab room. Stimuli were presented
489 using custom stimulus presentation software with millisecond timing precision. During testing, infant
490 participants were seated on their parent's laps in front of the screen at a distance of 70 cm. One
491 experimenter stood behind the presentation screen to monitor where the infant was looking. The visual
492 presentation was paused if the infant looked away from the screen and was continued when the infant
493 looked again at the center of the screen. To motivate infants to fixate and look at the screen, we
494 presented at the center of the screen small (~1°) colored cartoon images such as butterflies, flowers,
495 and ladybugs. They were presented in random order with durations uniformly distributed between 1
496 and 1.5 s. For adults, we used a fixation cross of the same size instead of the cartoons and asked the
497 participants to fixate and indicate when the fixation's color changed by pressing a space bar key on a
498 keyboard. EEG measurements for infant participants continued until the infant no longer attended the
499 screen and we obtained between 2-12 different 70-s sequences per individual. For adult participants, we
500 acquired 12 sequences per individual.

501 A frequency-tagging paradigm[23,46] was used to measure brain responses. In the experiment,
502 randomly selected images from 5 categories were presented sequentially at a rate of 4.286 Hz (~233 ms
503 per image) with no inter stimulus interval during each 70-s sequence. For each condition, one category

504 was determined as the target category; for this category random selected images from that category
505 were presented first and followed by four images randomly drawn from the other four categories with
506 no regular order (**Fig 1A)**. The target images are therefore presented periodically at 0.857 Hz (i.e. 4.286
507 Hz/5), but the intervals between sequential presentations of images from the other 4 categories was not
508 periodic. The probability of image occurrences across categories was equal at 20%. The experiment had
509 five conditions, one for each of the following target categories: faces, limbs, corridors, characters, and
510 cars. Each 70-s experimental sequence was composed of five 14-s long conditions which included a
511 1.1667-s stimulus fade-in and a 1.1667-s stimulus fade-out. The order of the category conditions was
512 randomized within each 70-s sequence. No image was repeated within a sequence. Two presentation
513 frequencies were embedded in the experiment: (i) the image frequency (4.286 Hz), which is predicted to
514 elicit visual responses to all stimuli over occipital visual cortex, and, (ii) the category frequency (0.857
515 Hz), which is predicted to elicit a category-selective response over lateral occipital-temporal electrodes.

516 **EEG Acquisition**

517 EEG data were recorded at 500 Hz from a 128-channel EGI High-Density Geodesic Sensor Net. For
518 infants, the net was connected to a NetAmps 300 amplifier (Electrical Geodesics, Inc., Eugene, OR, USA).
519 For the adults, the net was connected to a NetAmps400 amplifier. The EEG recording was referenced
520 online to a single vertex (electrode Cz) and the channel impedance was kept below 50 KΩ.

521 **Pre-processing**

522 EEG recordings were down-sampled to 420 Hz and were filtered using a 0.03-50 Hz bandpass filter
523 with custom signal processing software. Artifact rejection was performed in two steps. For infants, first,
524 channels with more than 20% of samples exceeding a 100-150 µV amplitude threshold were replaced
525 with the average amplitude of its six nearest-neighbor channels. The continuous EEG signals were then
526 re-referenced to the common average of all channels and segmented into 1166.7-ms epochs (i.e.,
527 duration of five stimuli starting with a target category image followed with four images drawn from the
528 rest four categories). Epochs with more than 15% of time samples exceeding threshold (150 - 200 µV)
529 were excluded further on a channel-by-channel basis[78]. For adults, the two-step artifact rejection was
530 performed with different criteria as EEG response amplitudes are lower in adults than infants[78]. EEG
531 channels with more than 15% of samples exceeding a 30 µV amplitude threshold were replaced by the
532 average value of their neighboring channels. Then the EEG signals were re-referenced to the common
533 average of all channels and segmented into 1.1667-s epochs. Epochs with more than 10% of time
534 samples exceeding threshold (30 - 80 µV) were excluded on a channel-by-channel basis[79].

535 **Supplementary Table S2** shows the number of epochs (1.1667-s each) we acquired before and after
536 data pre-processing summing across all five categories. We used data after pre-processing for further
537 analyses. There was no significant difference in the number of pre-processed epochs across infant age-
538 groups ($F_{(3,57)} = 1.5$, $p = .2$).

539 The number of electrodes being interpolated for each age group were 10.0 $\pm$ 4.8 for 3-4-month-
540 olds, 9.9 $\pm$ 3.7 for 4-6-month-olds, 9.9 $\pm$ 3.9 for 6-8-month-olds, and 7.7 $\pm$ 4.7 for 12-15-month-olds.
541 There was no significant difference in the number of electrodes being interpolated across infant age-
542 groups ($F_{(3,55)} = 0.78$, $p = .51$).

543 **Univariate EEG analyses**

544 Both image update and categorical EEG visual responses are reported in the frequency and time
545 domain over three regions-of-interest (ROIs): two occipito-temporal ROIs (left occipitotemporal (LOT):
546 channels 57, 58, 59, 63, 64, 65 and 68; right occipitotemporal (ROT) channels: 90, 91, 94, 95, 96, 99, and
547 100) and one occipital ROI (channels 69, 70, 71, 74, 75, 76, 82, 83 and 89). These ROIs were selected a
548 priori based on a previously published study[51]. We further removed several channels in these ROIs for
549 two reasons: (1) Three outer rim channels (i.e., 73, 81, and 88) were not included in the occipital ROI for
550 further data analysis for both infant and adult participants because they were consistently noisy. (2)
551 Three channels (66, 72, and 84) in the occipital ROI, one channel (50) in the LOT ROI, and one channel
552 (101) in the ROT ROI were removed because they did not show substantial responses in the group-level
553 analyses.

554 ***Frequency domain analysis.*** Individual participant's preprocessed EEG signals for each stimulus
555 condition were averaged over two consecutive epochs (2.3334-s). The averaged time courses for each
556 participant were then converted to the frequency domain at a frequency resolution of 0.4286 Hz via a
557 Discrete Fourier Transform (DFT). The frequency bins of interest are at exactly every other bin in the
558 frequency spectrum. The real and imaginary Fourier coefficients for each of the categorical and image
559 update responses for each condition were averaged across participants (vector averaging) to obtain a
560 group-level estimate. The amplitudes of response were then computed from the coherently averaged
561 vector. Hotelling's T2 statistic [80] was used to test whether response amplitudes were significantly
562 different from zero. We used Benjamini's & Hochberg's false discovery rate (FDR) procedure to correct
563 for multiple comparisons.

564 *Image-update visual responses (image frequency):* The amplitude and phase of the evoked response
565 at the image presentation rate and its first 3 harmonics (4.286 Hz, 8.571 Hz, 12.857 Hz, and 17.143 Hz).

566 *Categorical responses (category frequency):* The amplitude and phase of the response at the
567 category repetition frequency and its second harmonic (0.857 Hz, 1.714 Hz) for each category condition.
568 ***Time domain analyses.*** Preprocessed time domain EEG signals of each participant were low-passed
569 filtered with a 30Hz cut-off. The raw EEG signals contain many components including categorical
570 responses 0.857 Hz and harmonics), general visual responses (4.286 Hz and harmonics) and noise. To
571 separate out the temporal waveforms of these two responses, we first transformed the epoch-averaged
572 (2.3334-s) time series of each condition into frequency domain using a DFT. Then, we used an inverse
573 DFT to transform back to the time domain keeping only the responses at the category frequency and its
574 harmonics, zeroing the other frequencies. The same approach was used to separate the visual responses
575 by using an inverse DFT transform of the responses at 4.286 Hz and harmonics.
576 ***Categorical responses.*** We kept responses at frequencies of interest (0.857 Hz and its harmonics up
577 to 30 Hz, excluding the harmonic frequencies that overlapped with the image frequency and its
578 harmonics) and zeroed responses in other frequencies. Then we applied an inverse Fourier transform to
579 transform the data to the time domain. We further segmented the time series into 1.1667-s epochs and
580 averaged across these epochs for each condition and individual. The mean and standard error across
581 participants were computed for each condition at each time-point.
582 ***Image update visual responses.*** A similar procedure was performed except that frequencies of
583 interest are 4.286 Hz and its harmonics, and the rest were zeroed. As temporal waveforms for image-
584 update responses were similar across different category conditions, we averaged waveforms across all
585 five conditions and report the mean response (**Fig 2**).
586 ***Statistical analyses.*** To determine time windows in which amplitudes were significantly different
587 from zero for each condition, we used a cluster-based nonparametric permutation t-test, 10000
588 permutations, with a threshold of $p < 0.05$, two-tailed) on the post-stimulus onset time points (0-1167
589 ms) [81,82]. The null hypothesis is that the evoked waveforms are not different from zero at any time point.
590 For each permutation, we assigned random signs to the data of individual participants and computed
591 the group-level difference against zero using a t-test. We then calculated the cluster-level statistic as the
592 sum of t-values in the consecutive time points with p-values less than 0.05[83]. We calculated the
593 maximum cluster-level statistic for each permutation to generate a non-parametric reference
594 distribution of cluster-level statistics. We rejected the null hypothesis if the cluster-level statistic for any
595 consecutive time points in the original data was larger than 97.5% or smaller than 2.5% of the values in
596 the null distribution.
597 **Decoding analyses**

598 ***Group-level.*** We used a leave-one-out-cross-validation (LOOCV) classifier to test if spatiotemporal
599 responses patterns to each of the five categories were reliable across participants. The classifier was
600 trained on averaged data from N-1 participants and tested on how well it predicted the category the
601 left-out participant was viewing from their brain activations. This procedure was repeated for each left-
602 out participant. We calculated the averaged category temporal waveform for each category across
603 channels of our three ROIs: 7 LOT, 9 occipital, and 7 ROT, as the exact location of the channels varies
604 across individuals. Then we concatenated the waveform from the three ROIs to form a spatiotemporal
605 response vector (**Fig 5A**). At each iteration, the LOOCV classifier computed the correlation between each
606 of the five category vectors from the left-out participant (test data, for an unknown stimulus) and each
607 of the mean spatiotemporal vectors across the N-1 participants (training data, labeled data). The
608 winner-take-all (WTA) classifier classifies the test vector to the category of the training vector that yields
609 the highest correlation with the training vector (**Fig 5A**). For a given test pattern, correct classification
610 yields a score of 1 and an incorrect classification yields a score of 0. For each left-out infant, we
611 computed the percentage correct across all categories, and then the mean decoding performance across
612 all participants in an age group (**Fig 5B**).
613 ***Individual level.*** Similar to group level with 2 differences: (i) All analyses were done within an
614 individual using a split-half approach. That is, the classifier was trained on one half of the data (i.e., odd
615 or even trials) and tested on the other half of the data. (ii) Spatiotemporal patterns for each category
616 used the concatenated waveforms across 23 channels spanning the occipital and bilateral
617 occipitotemporal ROIs.
618 ***Category distinctiveness[10].*** Category distinctiveness is defined as the difference between the
619 similarity (correlation coefficient) of spatiotemporal responses within a category across odd and even
620 splits using different images and the average between-category similarity of spatiotemporal responses
621 across odd and even splits[10]. Distinctiveness is higher when the within category similarity is positive and
622 the between category similarity is negative and varies from -2 (no category information) to 2 (maximal
623 category information). We computed category distinctiveness for each of the 5 categories as in each
624 infant and determined if it varied from 3 to 15 months of age.
625 **Statistical Analyses of Developmental Effects**
626 To quantify developmental effects, we used linear mixed models (LMMs[84], with the 'fitlme' function
627 in MATLAB version 2021b (MathWorks, Inc.). LMMs allow explicit modeling of both within-subject
628 effects (e.g., longitudinal measurements) and between-subject effects (e.g., cross-sectional data) with
629 unequal number of points per participants, as well as examine main and interactive effects of both

630 continuous (age) and categorical (e.g., stimulus category) variables. We used random-intercept models
631 that allow the intercept to vary across participants (term: 1|participant). In all LMMs, we measured
632 development as a function of log 10(age in days) as development is typically faster earlier on. Indirect
633 evidence comes from neuroimaging and post-mortem studies showing that the structural development
634 of infants' brains is nonlinear, with development in the first two years being rapid, especially the first
635 year[73].
636 We report slope (rate of development), interaction effects, and their significance. Table 1
637 summarizes LMMs used in this study.
638
639

640 **Table 1. Linear mixed models (LMMs)**

Variable	LMM formula	Results
Peak latency: **latency of the peak waveform in each time window; window 1: 60-90 ms or window 2: 90-160 ms for 3-4-month-olds, and 90-110 ms for other age groups**	Peak latency ~ 1 + log10(age in days) × time window + (1|participant)	Fig 2G. Supplementary Table S4.
	Peak latency ~ 1+ log10(age in days) + (1|participant)	Fig 2H. Supplementary Table S5.
Category-selective response amplitude: **Root mean square (RMS) of category-selective response at category frequency (0.857 Hz) and its first harmonic (1.714 Hz)**	Response amplitude ~ 1+ log10(age in days) × category + (1|participant)	
Peak amplitude: **peak response in a 400-700ms time window**	Peak amplitude ~ 1+ log10(age in days) × category + (1|participant)	Supplementary Table S7.
	Peak amplitude ~ 1+ log10(age in days) + (1|participant)	Fig 4. Supplementary Table S8.
Category distinctiveness of spatiotemporal responses for each of the five categories	Category distinctiveness ~ log10(age in days) × category + (1|participant)	
	Category distinctiveness ~ log10(age in days) + (1|participant)	Fig 6B.

641

642 ***Analysis of Noise***

643 To test whether EEG noise levels vary with age, for example whether noise in the EEG data is larger
644 in the younger infants than older ones, we quantified the response amplitudes in the occipital ROI in the
645 frequency domain, at frequency bins next to the category and image frequency bins (white bars in **Fig**
646 **2A-D**, right panel). The noise level was quantified as the amplitude of response up to 8.571 Hz excluding
647 image presentation frequencies (4.286 Hz and harmonics) and category frequencies (0.857 Hz and
648 harmonics) as this frequency range includes the relevant main harmonics (**Fig 2E**). We used a LMM to
649 test if noise varies with age, with participant as a random effect:

650 **Noise amplitude ~ 1 + log10(age in days) + (1|participant)**

651 We found no significant differences in noise amplitude across infant age groups (**Fig 2E**, mean
652 amplitude across the first five noise bins: β_{age} = -.005, 95% CI: -.12 – .11, $t_{(59)}$ = -.09, p = .93; mean noise

across the first 10 bins: β_{age} = .04, 95% CI: -.03 – .12, $t_{(59)}$ = 1.16, p = .25, linear mixed models, LMMs, with age (log transformed) as fixed effects and participant as a random effect).

Data availability

Individual EEG data, and code for all analyses are available on Github: https://github.com/VPNL/InfantObjectCategorization.

Acknowledgements

This work was supported by grants from the Wu Tsai Neurosciences Institute of Stanford University, the Human Centered Artificial Intelligence Institute of Stanford University to KGS and AMN.

Author contributions

XY designed the experiment, coded the analysis pipeline, collected the data, analyzed data, and wrote the paper. AMN designed the experimental protocol and provided funding and instrumentation. SF and BF recruited the participants. ST, BF, and YC collected the data. ST and BF equally contributed to the study. KGS designed the experiment, oversaw the data collection and analyses, provided funding, and wrote the paper. All authors read the manuscript, provided critical revisions and approved the final paper for submission.

Competing interests

The authors declare no competing interests.

674 **References**

675 1. Thorpe, S., Fize, D. & Marlot, C. Speed of processing in the human visual system. *Nature*
676 **381**, 520–522 (1996).
677 2. Grill-Spector, K. & Kanwisher, N. Visual Recognition: As Soon as You Know It Is there, You
678 Know What It Is. *Psychological Science* **16**, (2005).
679 3. Grill-Spector, K. & Weiner, K. S. The functional architecture of the ventral temporal cortex
680 and its role in categorization. *Nat Rev Neurosci* **15**, 536–548 (2014).
681 4. Bugatus, L., Weiner, K. S. & Grill-Spector, K. Task alters category representations in
682 prefrontal but not high-level visual cortex. *Neuroimage* **155**, 437–449 (2017).
683 5. Nordt, M. *et al.* Cortical recycling in high-level visual cortex during childhood development.
684 *Nat Hum Behav* **5**, 1686–1697 (2021).
685 6. Margalit, E. *et al.* Ultra-high-resolution fMRI of Human Ventral Temporal Cortex Reveals
686 Differential Representation of Categories and Domains. *J. Neurosci.* **40**, 3008–3024 (2020).
687 7. Gomez, J. *et al.* Microstructural proliferation in human cortex is coupled with the
688 development of face processing. **355**, (2017).
689 8. Stigliani, A., Weiner, K. S. & Grill-Spector, K. Temporal Processing Capacity in High-Level
690 Visual Cortex Is Domain Specific. *Journal of Neuroscience* **35**, 12412–12424 (2015).
691 9. Haxby, J. V. *et al.* Distributed and Overlapping Representations of Faces and Objects in
692 Ventral Temporal Cortex. *Science* **293**, 2425–2430 (2001).
693 10. Nordt, M. *et al.* Longitudinal development of category representations in ventral temporal
694 cortex predicts word and face recognition. *Nat Commun* **14**, 8010 (2023).

11. Kanwisher, N., McDermott, J. & Chun, M. M. The Fusiform Face Area: A Module in Human Extrastriate Cortex Specialized for Face Perception. *The Journal of Neuroscience* **17**, 4302–4311 (1997).
12. Epstein, R. & Kanwisher, N. A cortical representation of the local visual environment. *Nature* **392**, 598–601 (1998).
13. Downing, P. E., Jiang, Y., Shuman, M. & Kanwisher, N. A Cortical Area Selective for Visual Processing of the Human Body. *Science* **293**, 2470–2473 (2001).
14. Golarai, G. *et al.* Differential development of high-level visual cortex correlates with category-specific recognition memory. *Nature Neuroscience* **10**, 512–522 (2007).
15. Scherf, K. S., Behrmann, M., Humphreys, K. & Luna, B. Visual category-selectivity for faces, places and objects emerges along different developmental trajectories. *Developmental Science* **10**, F15–F30 (2007).
16. Dehaene-Lambertz, G., Monzalvo, K. & Dehaene, S. The emergence of the visual word form: Longitudinal evolution of category-specific ventral visual areas during reading acquisition. *PLOS Biology* **16**, e2004103 (2018).
17. Spriet, C., Abassi, E., Hochmann, J.-R. & Papeo, L. Visual object categorization in infancy. *Proc. Natl. Acad. Sci. U.S.A.* **119**, e2105866119 (2022).
18. Mondloch, C. J. *et al.* Face Perception During Early Infancy. *Psychol Sci* **10**, 419–422 (1999).
19. Quinn, P. C., Eimas, P. D. & Rosenkrantz, S. L. Evidence for Representations of Perceptually Similar Natural Categories by 3-Month-Old and 4-Month-Old Infants. *Perception* **22**, 463–475 (1993).

716 20. Younger, B. A. & Fearing, D. D. Parsing Items into Separate Categories: Developmental
717 Change in Infant Categorization. *Child Development* **70**, 291–303 (1999).
718 21. Conte, S., Richards, J. E., Guy, M. W., Xie, W. & Roberts, J. E. Face-sensitive brain responses
719 in the first year of life. *NeuroImage* **211**, 116602 (2020).
720 22. Farzin, F., Hou, C. & Norcia, A. M. Piecing it together: Infants' neural responses to face and
721 object structure. *Journal of Vision* **12**, 6 (2012).
722 23. de Heering, A. & Rossion, B. Rapid categorization of natural face images in the infant right
723 hemisphere. *eLife* **4**, e06564 (2015).
724 24. Bayet, L. *et al.* Temporal dynamics of visual representations in the infant brain.
725 *Developmental Cognitive Neuroscience* **45**, 100860 (2020).
726 25. Xie, S. *et al.* Visual category representations in the infant brain. *Current Biology* **32**, 5422-
727 5432.e6 (2022).
728 26. Deen, B. *et al.* Organization of high-level visual cortex in human infants. *Nat Commun* **8**,
729 13995 (2017).
730 27. Kosakowski, H. L. *et al.* Selective responses to faces, scenes, and bodies in the ventral visual
731 pathway of infants. *Current Biology* **32**, 265-274.e5 (2022).
732 28. Kanwisher, N. Functional specificity in the human brain: A window into the functional
733 architecture of the mind. *Proceedings of the National Academy of Sciences* **107**, 11163–
734 11170 (2010).
735 29. Sugita, Y. Innate face processing. *Current Opinion in Neurobiology* **19**, 39–44 (2009).
736 30. Mahon, B. Z. & Caramazza, A. What drives the organization of object knowledge in the
737 brain? *Trends in Cognitive Sciences* **15**, 97–103 (2011).

738 31. Bi, Y., Wang, X. & Caramazza, A. Object Domain and Modality in the Ventral Visual Pathway.
739 *Trends in Cognitive Sciences* **20**, 282–290 (2016).
740 32. Behrmann, M. & Plaut, D. C. A vision of graded hemispheric specialization. *Ann N Y Acad Sci*
741 **1359**, 30–46 (2015).
742 33. Pascalis, O., de Schonen, S., Morton, J., Deruelle, C. & Fabre-Grenet, M. Mother's face
743 recognition by neonates: A replication and an extension. *Infant Behavior & Development*
744 **18**, 79–85 (1995).
745 34. Johnson, M. H., Dziurawiec, S., Ellis, H. & Morton, J. Newborns' preferential tracking of face-
746 like stimuli and its subsequent decline. *Cognition* **40**, 1–19 (1991).
747 35. Buiatti, M. *et al.* Cortical route for facelike pattern processing in human newborns.
748 *Proceedings of the National Academy of Sciences* **116**, 4625–4630 (2019).
749 36. Dehaene, S. *et al.* How Learning to Read Changes the Cortical Networks for Vision and
750 Language. *Science* **330**, 1359–1364 (2010).
751 37. Arcaro, M. J., Schade, P. F. & Livingstone, M. S. Universal Mechanisms and the Development
752 of the Face Network: What You See Is What You Get. *Annu Rev Vis Sci* **5**, 341–372 (2019).
753 38. Scott, L. S. & Arcaro, M. J. A domain-relevant framework for the development of face
754 processing. *Nat Rev Psychol* **2**, 183–195 (2023).
755 39. Livingstone, M. S. *et al.* Development of the macaque face-patch system. *Nat Commun* **8**,
756 14897 (2017).
757 40. Arcaro, M. J., Schade, P. F., Vincent, J. L., Ponce, C. R. & Livingstone, M. S. Seeing faces is
758 necessary for face-domain formation. *Nat Neurosci* **20**, 1404–1412 (2017).

759 41. Fausey, C. M., Jayaraman, S. & Smith, L. B. From faces to hands: Changing visual input in the
760 first two years. *Cognition* **152**, 101–107 (2016).
761 42. Jayaraman, S., Fausey, C. M. & Smith, L. B. Why are faces denser in the visual experiences of
762 younger than older infants? *Developmental Psychology* **53**, 38–49 (2017).
763 43. Allen, E. J. *et al.* A massive 7T fMRI dataset to bridge cognitive neuroscience and artificial
764 intelligence. *Nat Neurosci* **25**, 116–126 (2022).
765 44. Lerma-Usabiaga, G., Carreiras, M. & Paz-Alonso, P. M. Converging evidence for functional
766 and structural segregation within the left ventral occipitotemporal cortex in reading.
767 *Proceedings of the National Academy of Sciences* **115**, E9981–E9990 (2018).
768 45. Jagadeesh, A. V. & Gardner, J. L. Texture-like representation of objects in human visual
769 cortex. *Proceedings of the National Academy of Sciences* **119**, e2115302119 (2022).
770 46. Farzin, F., Hou, C. & Norcia, A. M. Piecing it together: Infants' neural responses to face and
771 object structure. *Journal of Vision* **12**, 6 (2012).
772 47. Heinrich, S. P., Mell, D. & Bach, M. Frequency-domain analysis of fast oddball responses to
773 visual stimuli: A feasibility study. *International Journal of Psychophysiology* **73**, 287–293
774 (2009).
775 48. Liu-Shuang, J., Norcia, A. M. & Rossion, B. An objective index of individual face
776 discrimination in the right occipito-temporal cortex by means of fast periodic oddball
777 stimulation. *Neuropsychologia* **52**, 57–72 (2014).
778 49. Rekow, D. *et al.* Odor-driven face-like categorization in the human infant brain. *Proceedings*
779 *of the National Academy of Sciences* **118**, e2014979118 (2021).

780 50. Taylor, M. J., McCarthy, G., Saliba, E. & Degiovanni, E. ERP evidence of developmental
781 changes in processing of faces. *Clinical Neurophysiology* **110**, 910–915 (1999).
782 51. Xie, W., McCormick, S. A., Westerlund, A., Bowman, L. C. & Nelson, C. A. Neural Correlates
783 of Facial Emotion Processing in Infancy. *Dev Sci* **22**, e12758 (2019).
784 52. Gentile, F. & Rossion, B. Temporal frequency tuning of cortical face-sensitive areas for
785 individual face perception. *NeuroImage* **90**, 256–265 (2014).
786 53. Retter, T. L., Jiang, F., Webster, M. A. & Rossion, B. All-or-none face categorization in the
787 human brain. *NeuroImage* **213**, 116685 (2020).
788 54. Peykarjou, S. Frequency tagging with infants: The visual oddball paradigm. *Front. Psychol.*
789 **13**, 1015611 (2022).
790 55. Guy, M. W., Zieber, N. & Richards, J. E. The Cortical Development of Specialized Face
791 Processing in Infancy. *Child Dev* **87**, 1581–1600 (2016).
792 56. Halit, H., Csibra, G., Volein, Á. & Johnson, M. H. Face-sensitive cortical processing in early
793 infancy. *Journal of Child Psychology and Psychiatry* **45**, 1228–1234 (2004).
794 57. Goren, C. C., Sarty, M. & Wu, P. Y. Visual following and pattern discrimination of face-like
795 stimuli by newborn infants. *Pediatrics* **56**, 544–549 (1975).
796 58. Halit, H., de Haan, M. & Johnson, M. H. Cortical specialisation for face processing: face-
797 sensitive event-related potential components in 3- and 12-month-old infants. *NeuroImage*
798 **19**, 1180–1193 (2003).
799 59. Macchi Cassia, V., Kuefner, D., Westerlund, A. & Nelson, C. A. A behavioural and ERP
800 investigation of 3-month-olds' face preferences. *Neuropsychologia* **44**, 2113–2125 (2006).

801 60. Tzourio-Mazoyer, N. *et al.* Neural Correlates of Woman Face Processing by 2-Month-Old
802 Infants. *NeuroImage* **15**, 454–461 (2002).
803 61. Rossion, B. Biomarkers of Face Perception in Autism Spectrum Disorder: Time to Shift to
804 Fast Periodic Visual Stimulation With Electroencephalography? *Biological Psychiatry:*
805 *Cognitive Neuroscience and Neuroimaging* **5**, 258–260 (2020).
806 62. Vettori, S. *et al.* Reduced neural sensitivity to rapid individual face discrimination in autism
807 spectrum disorder. *NeuroImage: Clinical* **21**, 101613 (2019).
808 63. Farran, E. K. *et al.* Characterizing the neural signature of face processing in Williams
809 syndrome via multivariate pattern analysis and event related potentials. *Neuropsychologia*
810 **142**, 107440 (2020).
811 64. Kobayashi, M., Kakigi, R., Kanazawa, S. & Yamaguchi, M. K. Infants' recognition of their
812 mothers' faces in facial drawings. *Dev Psychobiol* **62**, 1011–1020 (2020).
813 65. Peelen, M. V., Fei-Fei, L. & Kastner, S. Neural mechanisms of rapid natural scene
814 categorization in human visual cortex. *Nature* **460**, 94–97 (2009).
815 66. Cantlon, J. F., Pinel, P., Dehaene, S. & Pelphrey, K. A. Cortical Representations of Symbols,
816 Objects, and Faces Are Pruned Back during Early Childhood. *Cerebral Cortex* **21**, 191–199
817 (2011).
818 67. Cohen, M. A. *et al.* Representational similarity precedes category selectivity in the
819 developing ventral visual pathway. *NeuroImage* **197**, 565–574 (2019).
820 68. Grotheer, M. *et al.* White matter myelination during early infancy is linked to spatial
821 gradients and myelin content at birth. *Nat Commun* **13**, 997 (2022).

822 69. Natu, V. S. *et al.* Infants' cortex undergoes microstructural growth coupled with myelination
823 during development. *Commun Biol* **4**, 1191 (2021).
824 70. Tooley, U. A., Bassett, D. S. & Mackey, A. P. Environmental influences on the pace of brain
825 development. *Nat Rev Neurosci* **22**, 372–384 (2021).
826 71. Adibpour, P. *et al.* Characterizing the temporal dynamics and maturation of resting-state
827 activity: an EEG microstate study in preterm and full-term infants. 2024.03.19.585608
828 Preprint at https://doi.org/10.1101/2024.03.19.585608 (2024).
829 72. Lebenberg, J. *et al.* Mapping the asynchrony of cortical maturation in the infant brain: A
830 MRI multi-parametric clustering approach. *NeuroImage* **185**, 641–653 (2019).
831 73. Gilmore, J. H., Knickmeyer, R. C. & Gao, W. Imaging structural and functional brain
832 development in early childhood. *Nat Rev Neurosci* **19**, 123–137 (2018).
833 74. Bannert, M. M. & Bartels, A. Visual cortex: Big data analysis uncovers food specificity.
834 *Current Biology* **32**, R1012–R1015 (2022).
835 75. Jain, N. Selectivity for food in human ventral visual cortex. *Communications Biology* **6**, 175
836 (2023).
837 76. Pennock, I. M. L. *et al.* Color-biased regions in the ventral visual pathway are food selective.
838 *Current Biology* **33**, 134-146.e4 (2023).
839 77. Willenbockel, V. *et al.* Controlling low-level image properties: The SHINE toolbox. *Behavior*
840 *Research Methods* **42**, 671–684 (2010).
841 78. Norcia, A. M., Pei, F. & Kohler, P. J. Evidence for long-range spatiotemporal interactions in
842 infant and adult visual cortex. *Journal of Vision* **17**, 12 (2017).

79. Kohler, P. J., Barzegaran, E., Norcia, A. M. & McCandliss, B. D. Parietal Contributions to Abstract Numerosity Measured with Steady State Visual Evoked Potentials. 2020.08.06.239889 Preprint at https://doi.org/10.1101/2020.08.06.239889 (2020).

80. Victor, J. D. & Mast, J. A new statistic for steady-state evoked potentials. *Electroencephalography and Clinical Neurophysiology* **78**, 378–388 (1991).

81. Appelbaum, L. G., Wade, A. R., Vildavski, V. Y., Pettet, M. W. & Norcia, A. M. Cue-Invariant Networks for Figure and Background Processing in Human Visual Cortex. *J. Neurosci.* **26**, 11695–11708 (2006).

82. Blair, R. C. & Karniski, W. An alternative method for significance testing of waveform difference potentials. *Psychophysiology* **30**, 518–524 (1993).

83. Maris, E. & Oostenveld, R. Nonparametric statistical testing of EEG- and MEG-data. *Journal of Neuroscience Methods* **164**, 177–190 (2007).

84. Bosker, R. & Snijders, T. Multilevel Analysis: An Introduction to Basic and Advanced Multilevel Modeling. 1–368 (2011).

85. Li, G. *et al.* Mapping longitudinal development of local cortical gyrification in infants from birth to 2 years of age. *J Neurosci* **34**, 4228–4238 (2014).

86. Grieve, P. G., Emerson, R. G., Fifer, W. P., Isler, J. R. & Stark, R. I. Spatial correlation of the infant and adult electroencephalogram. *Clinical Neurophysiology* **114**, 1594–1608 (2003).

87. Norcia, A. M. & Tyler, C. W. Spatial frequency sweep VEP: Visual acuity during the first year of life. *Vision Research* **25**, 1399–1408 (1985).

88. Norcia, A. M., Tyler, C. W. & Hamer, R. D. Development of contrast sensitivity in the human infant. *Vision Research* **30**, 1475–1486 (1990).

865 89. Norcia, A. M. Development of vision in infancy. in *Adler's Physiology of the Eye* 531–551
866 (Elsevier Health Sciences, 2011).
867

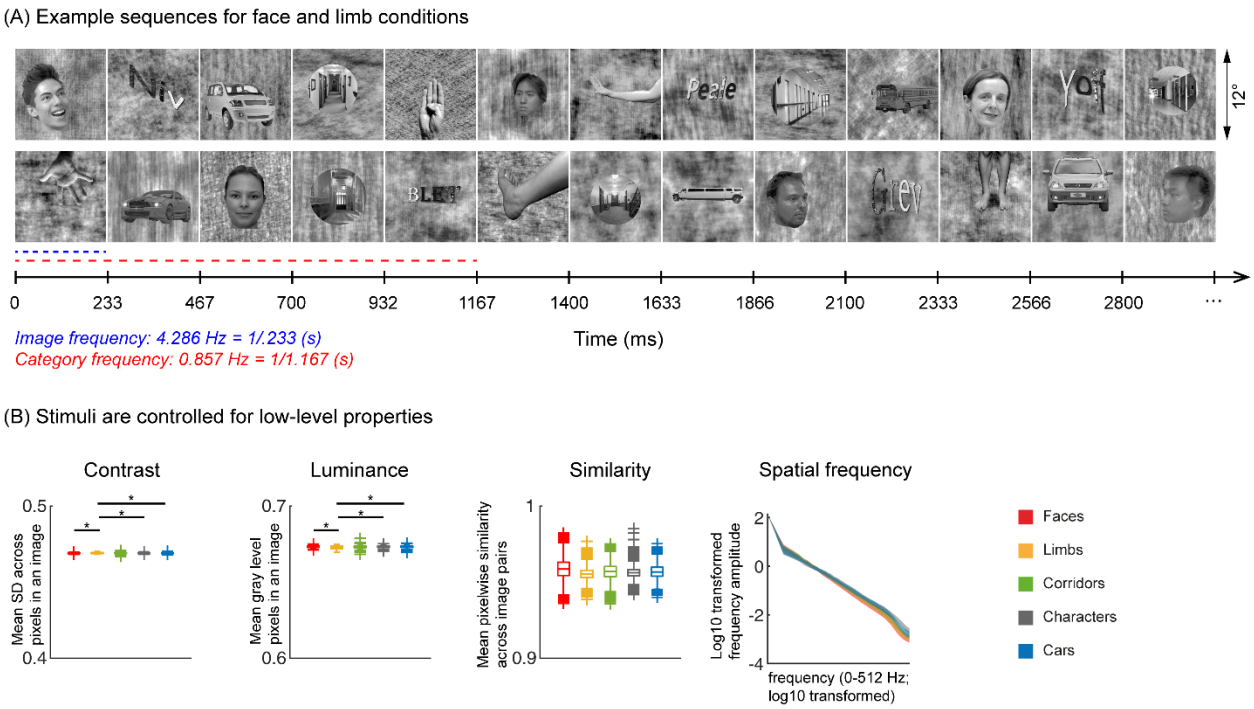

Figure 1. Experimental design and stimuli analysis. (A) Example segments of presentation sequences in which faces (top panel) and limbs (bottom panel) were the target category. Images spanning 12° containing gray-level images of items from different categories on a phase scrambled background appeared for 233 ms (frequency: 4.286 Hz). A different exemplar from a single category appeared every 5th image (frequency: 0.857 Hz). Between the target category images, randomly drawn images from the other four categories were presented. Sequences consisted of 20% images from each of the five categories and no images were repeated. Each category condition lasted for 14-s and contained 12 such cycles. Participants viewed in random order 5 category conditions: faces, limbs, corridors, characters, and cars forming a 70-s presentation sequence. (B) Images were controlled for several low-level properties using the SHINE toolbox as explained in [8]. Metrics are colored by category (see legend). *Contrast*: mean standard deviation of gray-level values in each image, averaged across 144 images of a category. *Luminance*: Mean gray-level of each image, averaged across 144 images of a category. *Similarity:* Mean pixel wise similarity between all pairs of images in a category. For all 3 metrics, boxplots indicate median, 25%, 75% percentiles, range, and outliers. Significant differences between categories are indicated by asterisks, for contrast and luminance (non-parametric permutation t-test $p < .05$, Bonferroni corrected); for image similarity, all categories are significantly different than others (non-parametric permutation testing, $p < 0.05$, Bonferroni corrected, except for corridors vs. cars, $p = .24$). *Spatial Frequency*: *Solid lines:* Distribution of spectral amplitude in each frequency averaged across 144 images in each category. *Shaded area*: standard deviation. Spatial frequency distributions are similar across categories.

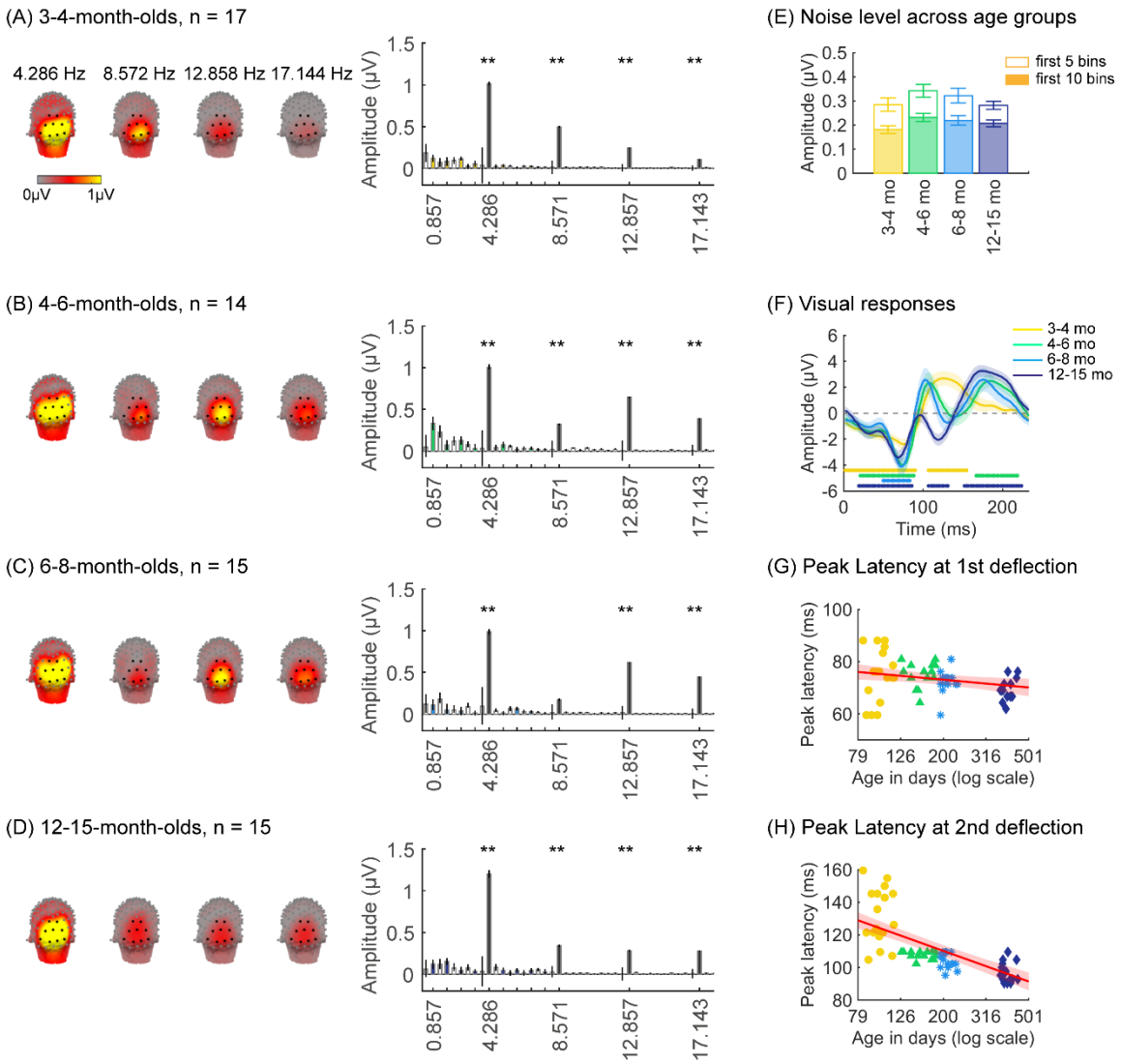

Figure 2. Strong visual responses over occipital cortex at the image-update frequency and its harmonics in all age groups. Each panel shows mean responses across infants in an age group. (A) 3-4-month-olds, n=17; (B) 4-6-month-olds, n=14; (C) 6-8-month-olds, n=15; (D) 12-15-month-olds, n=15. *Left panels in each row:* spatial distribution of the visual response at the image update frequency and its first three harmonics. *Middle panels in each row:* mean Fourier Amplitude Spectrum across 9 occipital electrodes of the occipital ROI showing high activity at harmonics of the image update frequency marked out by thicker lines. Data are first averaged in each participant and each condition and then across participants. *Error bars:* standard error of the mean across participants. *Asterisks:* Response amplitudes significantly larger than zero, $p < .01$, FDR corrected. *Colored bars:* amplitude of response at category frequency and its harmonics. *White bars:* amplitude of response at noise frequencies. (E) Noise amplitudes in the frequency range up to 8.571 Hz (except for the visual response frequencies and visual category response frequencies) from the amplitude spectra in (A) for each age group (white bars on the spectra). *Error bars:* standard error of the mean across participants. (F) Mean image-update response over occipital electrodes for each age group. Waveforms are cycle averages over the period of the individual image presentation time (233-ms). *Lines:* mean response. *Shaded areas:* standard error of the mean across participants of each group. *Horizontal lines colored by age group:* significant responses vs. zero ($p < .05$ with a cluster-based analysis, see Methods). (G) Peak latency for the first peak in the 60-90 ms interval after stimulus onset. Each dot is a participant; Dots are colored by age group. *Line*: linear mixed model (LMM) estimate of peak latency as a function of log10(age). *Shaded area:* 95% confidence interval (CI). (H) Same as (G) but for the second peak in the 90-160 ms interval for 3-4-month-olds, and 90-110 ms for older infants.

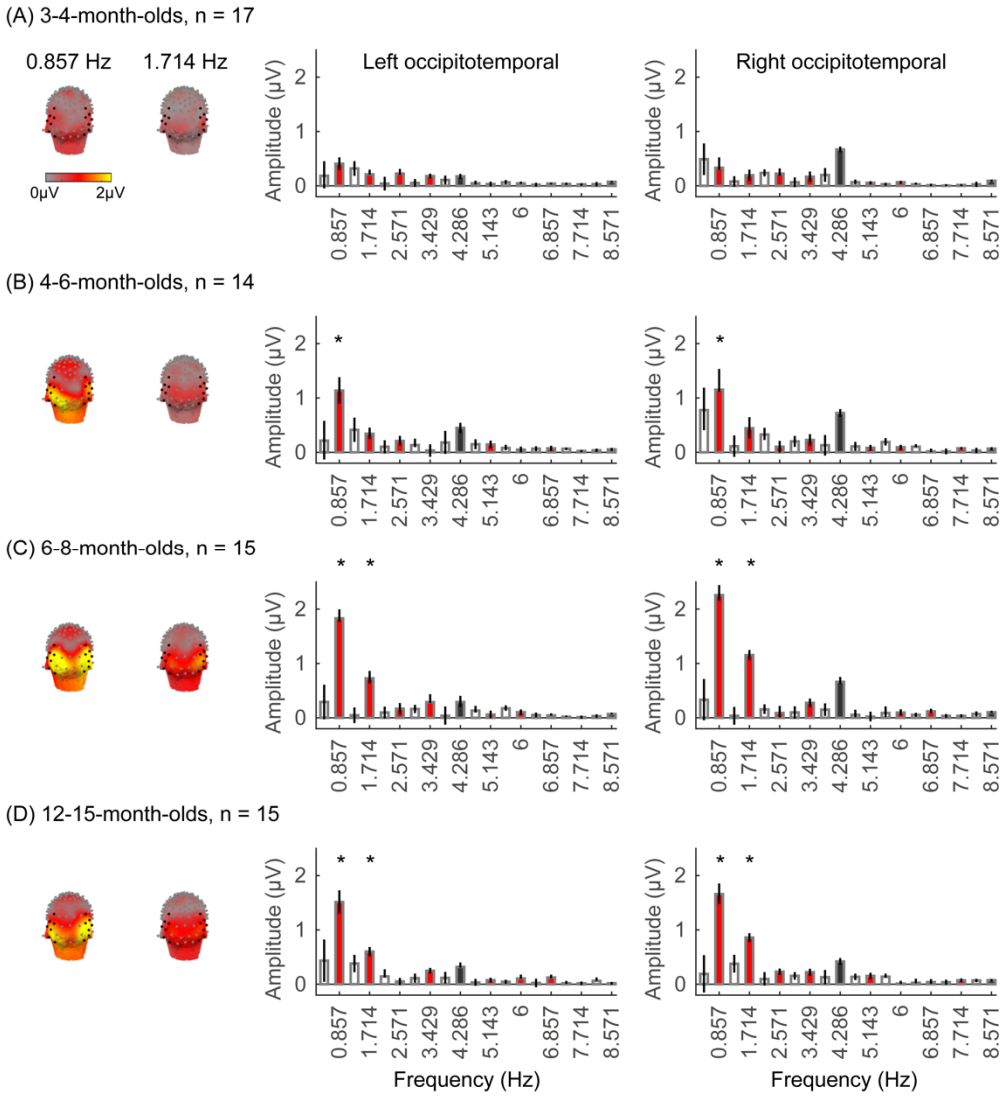

Figure 3. Face responses emerge over occipitotemporal electrodes after 4 months of age. Each panel shows mean responses at the category frequency and its harmonics across infants in an age group. (A) 3-4-month-olds, n=17; (B) 4-6-month-olds; n=14; (C) 6-8-month-olds, n=15; (D) 12-15-month-olds, n=15. Left panels in each row: spatial distribution of response to category frequency at the 0.857 Hz and its first harmonic. Harmonic frequencies are indicated on the top. Right two panels in each row: mean Fourier amplitude spectrum across two ROIS: 7 left and 7 right occipitotemporal electrodes (shown in black on the left panel). Data are first averaged across electrodes in each participant and then across participants. Error bars: standard error of the mean across participants of an age group. Asterisks: significant amplitude vs. zero ($p < .05$, FDR corrected at 2 levels). Black bars: image frequency and harmonics; Colored bars: category frequency and harmonics. White bars: noise frequencies. Responses for the other categories (limbs, corridors, characters and cars) in Supplementary Figures S5-S8.

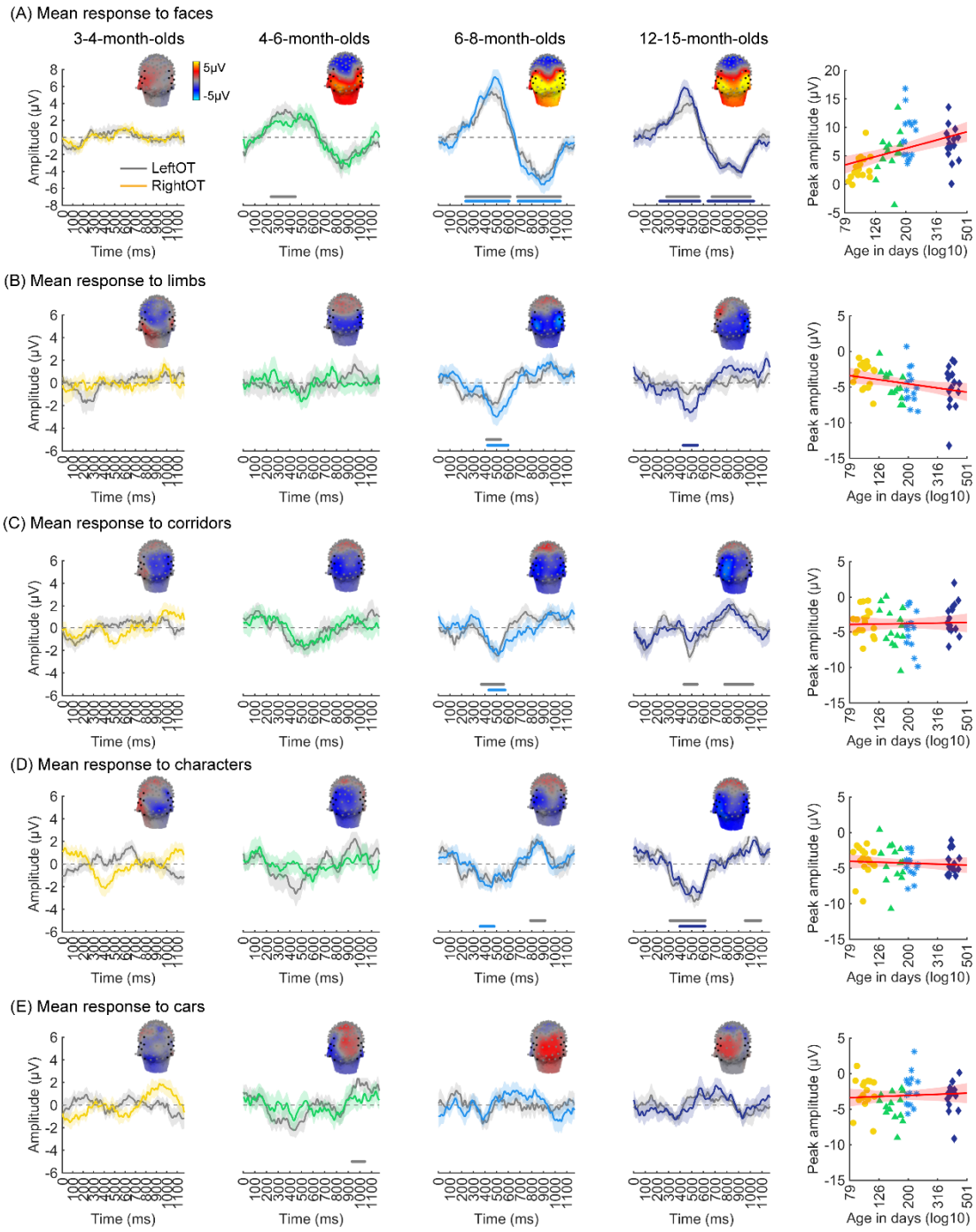

Figure 4. Temporal dynamics of category-selective responses as a function of age. Category-selective responses to (A) faces, (B) limbs, (C) corridors, (D) characters, and (E) cars over left and right occipitotemporal ROI. Data are averaged across electrodes of an ROI and across individuals. Left four panels in each row show the responses in the time domain for the four age groups. *Colored lines:* mean responses in the right occipitotemporal ROI. *Gray lines:* mean responses in the left occipitotemporal ROI. *Colored horizontal lines above x-axis:* significant responses relative to zero for the right OT ROI. *Gray horizontal lines above x-axis:* significant responses relative to zero for the left OT ROI. *Top*: 3-D topographies of the spatial distribution of the response to target category stimuli at a 483-500 ms time window after stimulus onset. *Right panel in each row:* amplitude of the peak deflection defined in a 400-700 ms time interval after stimulus onset. Each dot is a participant; Dots are colored by age group. *Red line:* linear mixed model (LMM) estimate of peak amplitude as a function of log10(age). *Shaded area:* 95% CI.

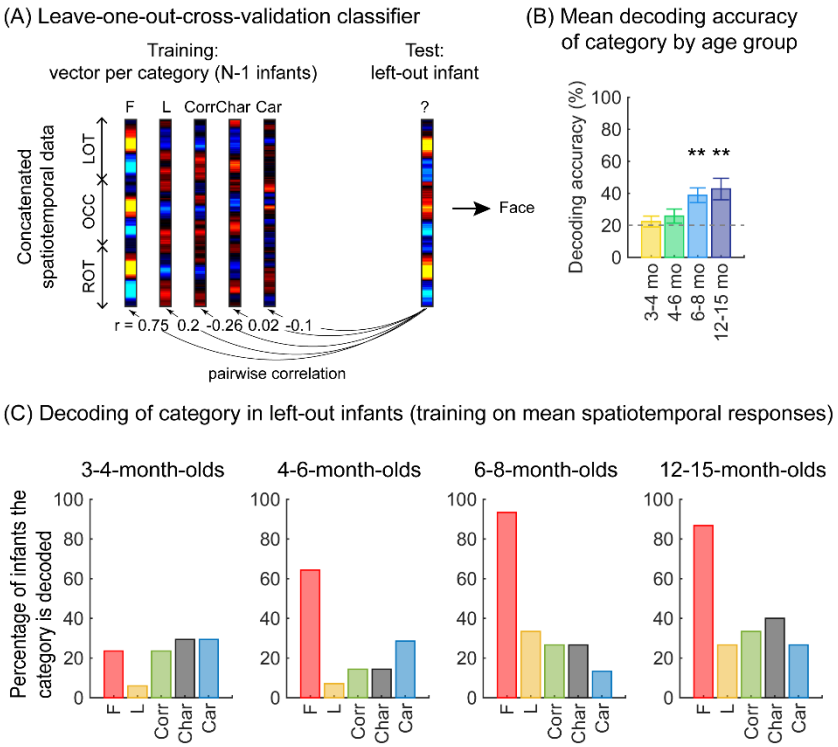

Figure 5. Successful decoding of faces from mean spatiotemporal responses starting from 4 months of age. (A) An illustration of winner-takes-all leave-one-out-cross validation (LOOCV) classifier from mean spatiotemporal response patterns of each category. Spatiotemporal patterns of response for each category are generated by concatenating the mean time courses from N-1 infants from three ROIs: left occipitotemporal (LOT), occipital (OCC), and right occipitotemporal (ROT). At each iteration, we train the classifier with the mean spatiotemporal patterns of each category from N-1 infants, and test how well it predicts the category the left-out infant is viewing from their spatiotemporal brain response. The winner-take-all (WTA) classifier determines the category based on the training vector that has highest pairwise correlation with the and test vectors. (B) Mean decoding accuracies across all five categories in each age group. *Asterisks:* significant decoding above chance level ($p < .01$, Bonferroni corrected, one-tailed). (C) Percentage of infants in each age group we could successfully decode for each category. *Dashed lines*: chance level.

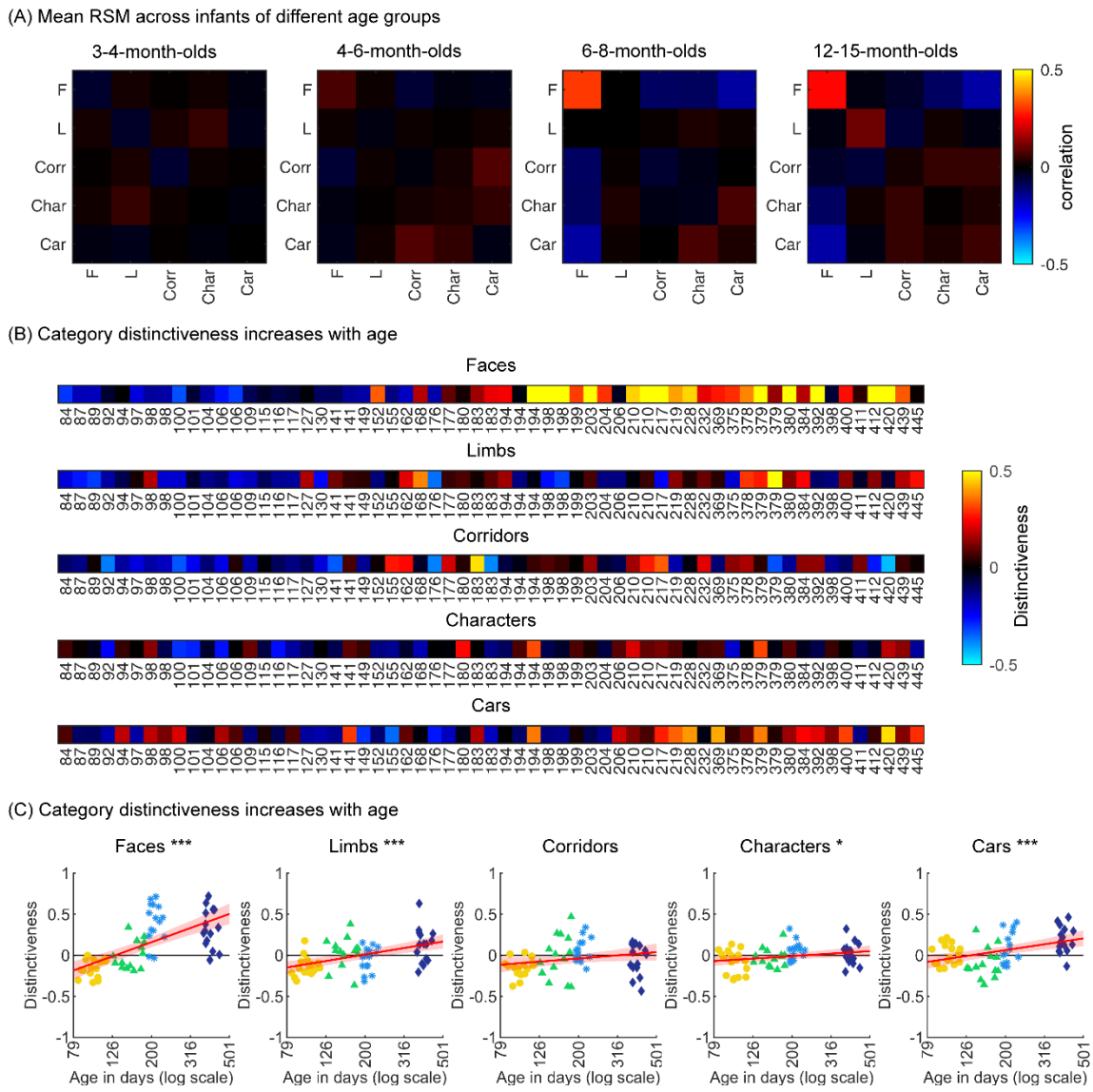

Figure 6. Individual split-half spatiotemporal pattern analyses reveal category information slowly emerges in the visual cortex after 6 months of age. (A) Representation similarity matrices (RSM) generated from odd/even split-halves of the spatiotemporal patterns of responses in individual infants. Spatiotemporal patterns for each category are generated by concatenating the mean time courses of each of 23 electrodes across left occipitotemporal (LOT), occipital (OCC), and right occipitotemporal (ROT). (B) Category distinctiveness calculated for each infant and category by subtracting the mean between-category correlation values from the within-category correlation value. (C) Distinctiveness as a function of age; panels by category; Each dot is a participant. Dots are colored by age group. *Red line:* linear mixed model (LMM) estimates of distinctiveness as a function of log10(age). *Shaded area:* 95% CI.

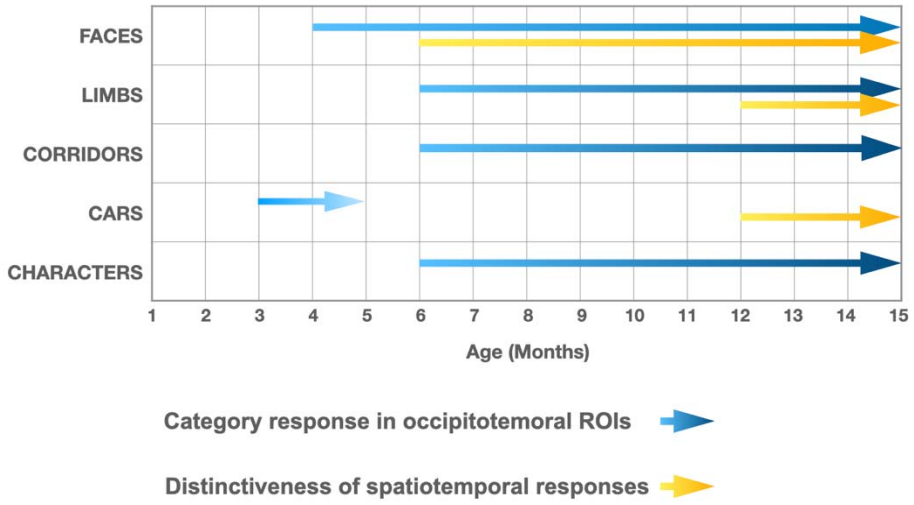

Figure 7. Selective responses to items of a category and distinctiveness in distributed patterns develop at different times during the first year of life. *Blue arrows*: presence of significant mean ROI category-selective responses in lateral occipital ROIs, combining results of analyses in the frequency and time domains. *Yellow arrows*: presence of significantly above zero distinctiveness in the distributed spatiotemporal response patterns across occipital and lateral occipital electrodes.

Supporting Information for
When Do Visual Category Representations Emerge in Infants' Brains?

Xiaoqian Yan[1,2,3], Sarah Tung[1+], Bella Fascendini[1+], Yulan Diana Chen[1,2], Anthony M. Norcia[1,2*], Kalanit Grill-Spector[1,2,4*]

1. Department of Psychology, Stanford University, Stanford, CA 94305, USA

2. Wu Tsai Neurosciences Institute, Stanford University, Stanford, CA 94305, USA

3. Institute of Science and Technology for Brain-Inspired Intelligence, Fudan University, Shanghai, China

4. Neurosciences Program, Stanford University, Stanford, CA 94305, USA

* co-senior-author

\+ equal contribution

Corresponding author: Xiaoqian Yan
Email: xqyan@fudan.edu.cn

This file includes:

- Supplementary Methods
- Supplementary Results
- Supplementary References
- Figures S1 to S10
- Tables S1 to S9
- Legends for Movies S1 to S5

Supplementary Materials

1. Demographic information

Supplementary Table 1. Demographic Information.

	3-4 MONTHS (N = 17)	**4-6 MONTHS (N = 14)**	**6-8 MONTHS (N = 15)**	**12-15 MONTHS (N = 15)**
Age at test (days)	84 - 117	127 - 183	194 - 232	369 - 445
Sex				
Female	7	7	6	4
Male	10	7	9	11
Race				
White	5	4	6	5
Black				
Asian		1	1	2
Mixed races	11	8	6	7
Unknown	1	1	2	1

Supplementary Table 2. Average number of valid epochs summed across all five categories for each age group before and after data pre-processing.

	3-4 MONTHS (N = 17)	**4-6 MONTHS (N = 14)**	**6-8 MONTHS (N = 15)**	**12-15 MONTHS (N = 15)**	**ADULTS (N = 20)**
Before pre-processing	281 (± 103)	270 (± 86)	346 (±111)	324 (±78)	600 (± 0)
After pre-processing	223 (± 89)	219 (± 73)	266 (± 91)	269 (± 77)	560 (± 37)
Ratio (after/before)	79%	81%	77%	83%	93%

991 **2. Low-level image properties analyses**

992 As images of items of visual categories vary both on low-level and high-level properties, and both
993 the EEG signal and babies' attention may be affected by low-level properties like contrast or luminance,
994 it is important to control for several low-level factors such as luminance, contrast, similarity spatial
995 frequency, as well as high-level properties such as familiarity across categories. Here we used a subset of
996 categories from[8], that did not contain familiar stimuli to our participants and were controlled for several
997 low-level factors using the SHINE toolbox[77]. To validate the effect of employing SHINE, we evaluated
998 several low-level metrics and tested if they differed across categories: (i) *Luminance:* mean gray level of
999 each image; (ii) *Contrast:* mean standard deviation of gray level values of each image; (iii) *Similarity:*
1000 mean pixel-wise similarity between gray levels across pairs of images of a category, and (iv) *Spatial*
1001 *frequency distribution*: we transformed each image to the Fourier Domain using FFT and calculated its
1002 circular amplitude spectrum. We calculated these metrics for each image, then tested if contrast,
1003 luminance, similarity metrics were significantly different across categories using pairwise nonparametric
1004 permutation t-tests (10,000 times, with Bonferroni correction). While it is difficult to completely control
1005 multiple low-level metrics across categories[77], our analyses show that images are largely controlled for
1006 several low-level metrics across categories, and that medians, means, and ranges are matched across
1007 categories (**Fig 1B;** supplementary **Table 3**). With respect to differences in contrast and luminance, there
1008 are no significant differences across categories except that limbs have slightly but significantly lower
1009 luminance (*ps* < .05, Bonferroni corrected) and lower pairwise similarity (*ps* < .01) and higher contrast
1010 (*ps* < .05, except for corridors) than other categories. For similarity, the medians and ranges are similar
1011 across categories, but the outliers vary producing significant differences across categories (permutation
1012 tests, *p* < .05, Bonferroni corrected). For spatial frequency distribution, the means and standard
1013 deviations are similar across categories (Fig 1B-right). We further ran Kolmogrov-Smirnov tests for each
1014 pair of categories with Bonferroni correction, our results revealed significantly different distributions
1015 across category pairs (*ps* < .001, except for limbs and corridors).
1016

1017 **Supplementary Table 3. Mean (±SD) values of contrast, luminance and similarity metrics across**
1018 **images within each five stimuli categories.**

	Faces	**Limbs**	**Corridors**	**Characters**	**Cars**
Contrast	0.469 (2.533e-4)	0.391 (3.91e-4)	0.404 (4.04e-4)	0.2856 (2.856e-4)	0.3269 (3.269e-4)
Luminance	0.6733 (0.0007)	0.6729 (0.0011)	0.6732 (0.0011)	0.6732 (0.0008)	0.6733 (0.0009)
Similarity	0.9855 (0.0063)	0.9555 (0.0039)	0.9569 (0.0051)	0.9563 (0.0033)	0.9570 (0.0044)

1019
1020

1021 **3. Analyses of adult data**

1022 In the study, one concern is that the amount of empirical data typically collected in infants is less
1023 than in adults, which may compromise the experimental power to detect responses in infants as it may
1024 affect the noise-bandwidth (sensitivity) of the frequency tagging analysis. Thus, we tested whether it is
1025 possible to measure category-selective responses in 20 adults using the same experiment (**Fig 1**) and the
1026 same amount of data collected in infants using three types of analyses. By using the same number of
1027 trials in adults as those obtained from our infant participants for data analyses, our goal was to test that
1028 we had sufficient power to detect categorical responses from infants using the experimental paradigm.
1029 We expect temporal and amplitude differences between adults and infants[25] as infants have immature
1030 brains and skulls. For example, cortical gyrification, which determines the orientation of the electrical
1031 fields generated in a certain part of the brain region on the scalp, still undergoes development during

the first two years of infants' lives[85]. Second, adults' skulls are thicker and have lower conductivity than infants' skulls, thus electrical signals on their scalp are lower than infants[86]. Nonetheless, we tested if we could in principle detect category information in adults with the same amount of data as infants. We reasoned that if category information can be detected in adults and signals are stronger in infants then we should have the power to detect category information in infants.

Visual Responses: We averaged the preprocessed data across two consecutive epochs (2.3334-s) and across conditions for each individual to measure visual responses to all images that were presented at 4.286 Hz and then transformed the data to the frequency domain. Supplementary **Fig S1A** shows the three-D topographies of group-averaged responses at 4.286 Hz and its first 3 harmonics (left panel) and the group-averaged Fourier amplitude spectrum over middle occipital and occipitotemporal ROIs (right panel). We used Hotelling's T2 statistic to test the amplitude significance and found significant visual responses in adults at 4.286 Hz over the occipital ROI containing 9 electrodes over early visual cortex ($p < .05$, FDR corrected at 4 levels) and significant visual responses at 4.286 Hz and its first two harmonics over the occipitotemporal ROI (14 electrodes) (*ps* < .05).

Examining the temporal waveform of the visual response (filtered at the image frequency and its harmonics), we found a relatively slow waveform with one peak, after 100 ms since stimulus onset (Supplementary **Fig S1B**).

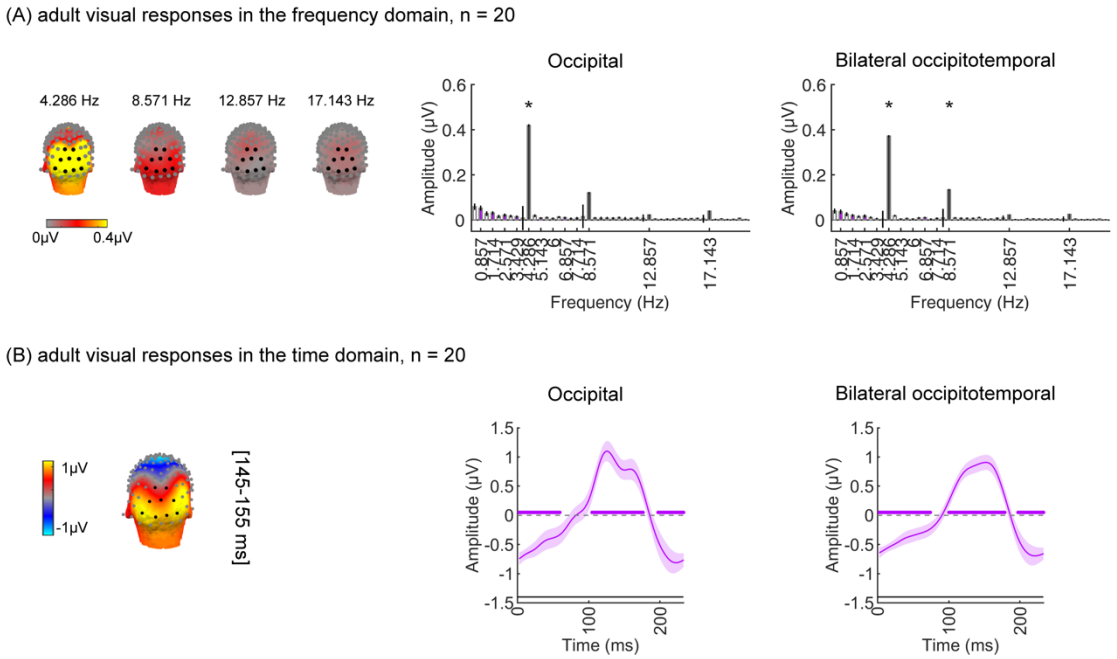

Supplementary Figure 1. Robust visual and categorical responses recorded over occipitotemporal and occipital cortex in 20 adults. (A) *Left panel:* spatial distribution of visual response at 4.286 Hz and harmonic. Harmonic frequencies are indicated on the top. *Right panel:* mean Fourier amplitude spectrum across 14 electrodes in the occipitotemporal and 9 electrodes in the occipital ROIs. *Error bars:* standard error of the mean across participants. *Black bars:* image frequency and harmonics; Purple bars: category frequency and harmonics; Asterisks: significant response amplitude from zero at $p_{FDR} < .05$. (B) *Left:* spatial distribution of visual responses at time window 145-155 ms. Right: Mean visual responses over two ROIs in the time domain. Waveforms are shown for a time-window of 233-ms during which 1 image is shown. *Shaded area*: standard error of the mean across participants. Blank line at around y = -1.5: stimulus onset duration. To define time windows in which amplitudes were significantly different from zero, we used a cluster-based nonparametric permutation t-test (1000 permutations, with a threshold of $p < 0.05$, two-tailed) on the post-stimulus onset time-points (0-1167 ms)[81,82].

1063 ***Visual Category responses:*** As adults have mature category-selective regions, we next tested if
1064 using our SSVEP paradigm and the same amount of data as in infants, we identify significant category-
1065 selective responses in adults. First, we analyzed the mean response at the category frequency and its
1066 harmonics in lateral occipitotemporal regions of interest (ROIs). This is a selective response as it reflects
1067 the relative response to the target category (generalized across exemplars) above the general visual
1068 response to images of other categories. Despite lower response amplitudes in adults than infants, using
1069 the same amount of data as infants, adults show significant category-selective responses to each of
1070 these five categories (Supplementary **Fig S2A** for all categories). Supplementary **Fig S2A** shows the
1071 group-averaged Fourier amplitude spectrum over left and right occipitotemporal ROIs (top panels) and
1072 the three-D topographies of group-averaged responses at 0.857 Hz and its first harmonic (bottom panel).
1073 We used Hotelling's T2 statistic to test the amplitude significance and found significant above-zero
1074 category-selective responses in adults at 0.857Hz and its multiple harmonics over bilateral
1075 occipitotemporal ROIs containing 7 electrodes each ($ps < .05$, FDR corrected over 8 levels).

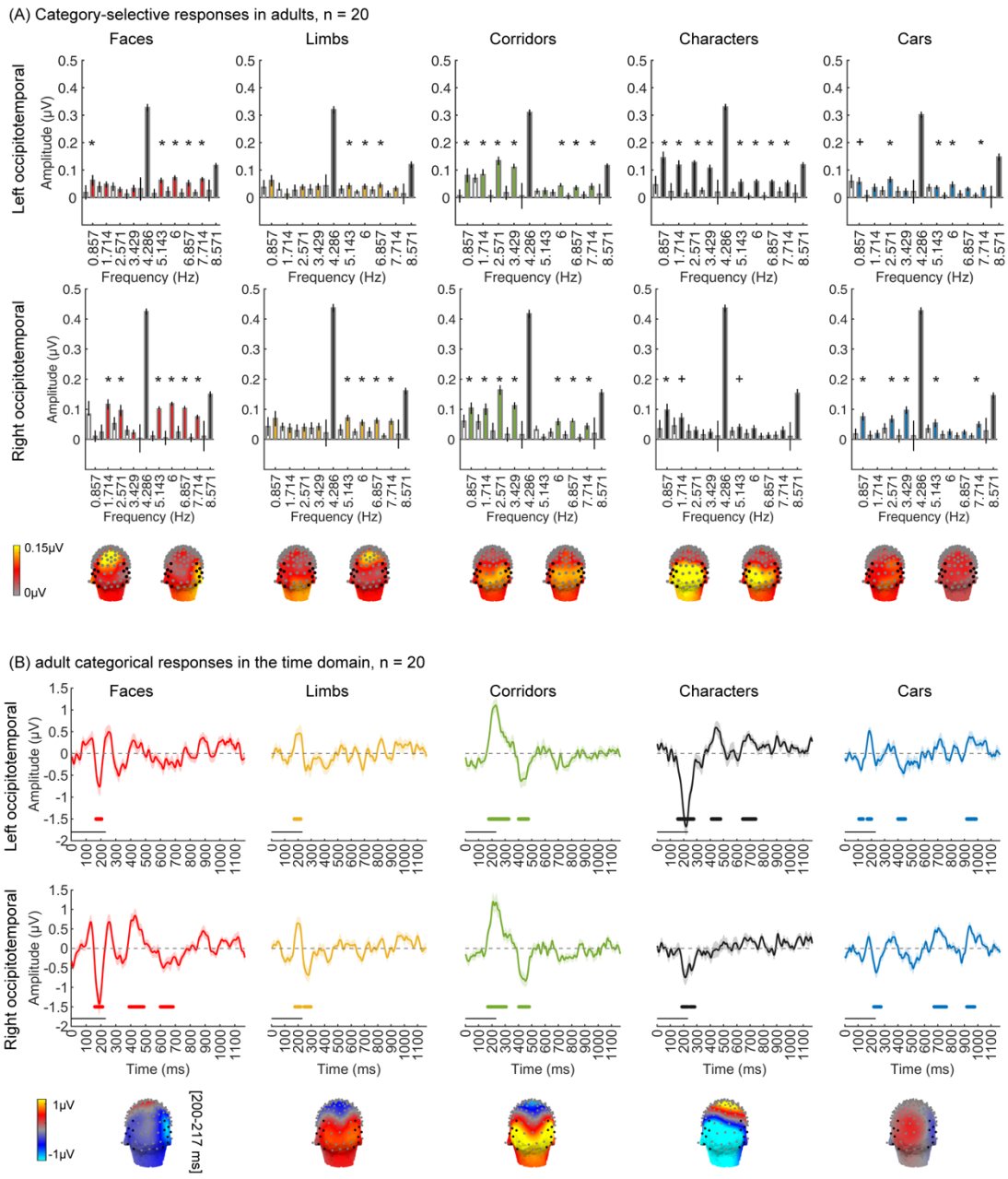

Supplementary Figure 2. Adult control: using the same amount of data as infants reveals strong category-selective responses in adults' occipitotemporal cortex. (A) Mean Fourier Amplitude Spectrum across 7 (left OT: 57, 58, 59, 63, 64, 65, 68; Right OT: 90, 91, 94, 95, 96, 99) electrodes in bilateral occipitotemporal ROIs. Data are first averaged in each participant and then across 20 participants. *Error bars*: standard error of the mean across participants. *Black bars*: visual response at image frequency and harmonics; *Colored bars:* categorical response at category frequency and harmonics. *Asterisks:* significant response amplitude from zero at $p_{FDR} < .05$ for category harmonics. Crosses: significant response amplitude from zero at $p < .05$ with no FDR correction. *Black dots:* ROI channels used in analysis. (B) Mean category-selective responses in the time domain. Data are averaged across electrodes of each of the left and right occipitotemporal ROI in each participant and then across participants. *Colored lines along x-axis at y = -1.5:* significant deflections against zero (calculated with a cluster-based method, see methods part). *Black line above x-axis:* stimulus onset duration. *Bottom panel:* spatial distribution of category-selective responses at time window 200-217 ms.

By transforming the filtered data at the category frequency and its harmonics to examine the temporal waveform of each category. Notably, each category generates a unique topography (bottom panels) at 200-217 ms after stimulus onset (Supplementary **Fig 2B**). For faces, we found an early negative deflection peaking ~200 ms after stimulus onset in both the left and right occipitotemporal ROIs, with the right occipitotemporal ROI showing a numerically larger mean response amplitude than the left (Supplementary **Fig S2B-**faces). Similarly, we found an early negative peak at around 200 ms for characters, and a left hemisphere dominance (at the 162-248 ms and 398-474 ms time windows (Supplementary **Fig S2B**-characters). For both limbs and corridors, there was an early positive waveform peaking at around 200 ms in both hemispheres with no hemispheric differences.

Second, we examined in the same 20 adults whether the spatiotemporal pattern of brain responses evoked by different visual categories are distinct from one another and are reliable across participants, using a leave-one-out-cross-validation (LOOCV) classifier approach with spatiotemporal timeseries concatenated with mean temporal waveforms from 3 ROIs: (Supplementary **Fig 3A-left**). Mean LOOCV classification performance was around 80% and significantly above chance in adults (Supplementary **Fig 3A-right**). This classification was associated with correct decoding of all 5 categories from distributed responses in the majority of participants.

Third, we examined in the same 20 adults if there is reliable category information in spatiotemporal distributed responses in each individual. Distributed spatiotemporal responses were measured in individual participants over 23 occipital and lateral occipital ROIs using split half of data. We computed the representations similarity matrix (RSM) across split halves and then calculated category distinctiveness by subtracting mean between category similarity from within category similarity for each category. Mean RSM across 20 adults shows that spatiotemporal patterns are more similar across items of a category than across items of different categories (Supplementary **Fig 3B-left**), and the category distinctiveness scores are significantly above zero for all five categories: faces, $t_{(19)} = 11.18$, $p_{FDR} < .05$; limbs, $t_{(19)} = 5.01$, $p_{FDR} < .05$; corridors, $t_{(19)} = 5.58$, $p_{FDR} < .05$; characters, $t_{(19)} = 6.56$, $p_{FDR} < .05$; and cars, $t_{(19)} = 10.59$, $p_{FDR} < .05$.

Together, these analyses suggest that the experimental paradigm has sufficient power to identify category representations both at the group and individual levels.

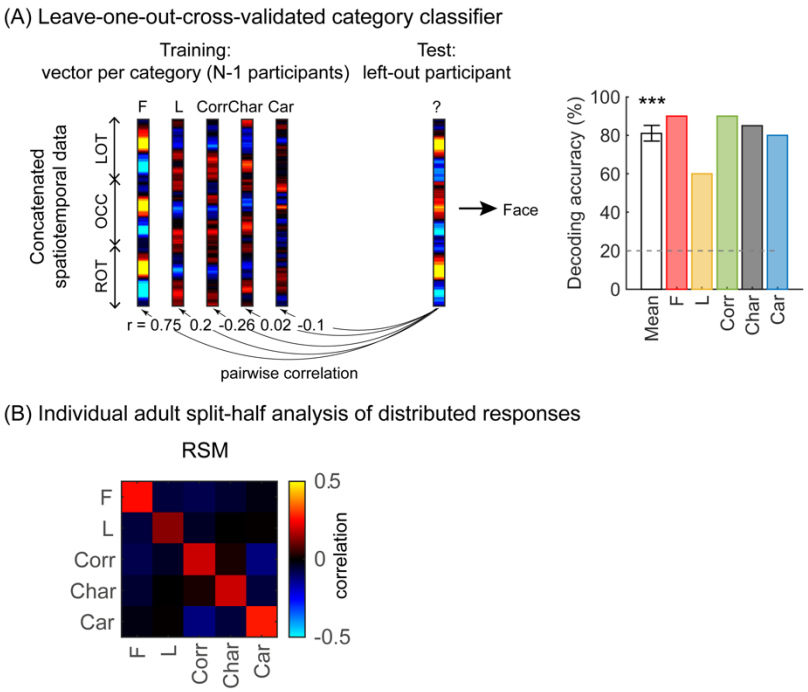

Supplementary Figure 3: Adult control: using the same amount of data as infants reveals distributed category-selective responses in adults' occipitotemporal cortex. (A) *Left:* An illustration of winner-takes-all leave-one-out-cross-validated classifier (LOOCV) using the spatiotemporal response patterns of each category. Spatiotemporal patterns of response for each category are generated by concatenating the mean time courses from each of the three ROIs: left occipitotemporal (LOT), occipital (OCC), and right occipitotemporal (ROT). At each iteration, we train the classifier with the mean spatiotemporal patterns of each category from N-1 participants, and test how well it predicts the category the left-out participant is viewing from their spatiotemporal brain response. This is a winner-take-all classifier which predicts the category based on the highest pairwise correlation between the training and testing vectors. *Right: White:* mean decoding accuracy across all five categories. In adults, this is significantly above chance level ($t_{(19)} = 15.4$, $p < .001$). *Colored:* decoding accuracy per category. (B) *Left:* Average adult representation similarity matrix (RSM) for odd/even splits of spatiotemporal patterns of categorical over 23 electrodes in the LOT, OCC, ROT. RSMs were generated in each participant and then averaged across all participants. *Diagonal:* correlation of distributed responses across different exemplars of the same category; *Off-diagonal:* correlations across different exemplars from different categories. *Acronyms:* F: faces; L: limbs; Corr: corridors; Char: characters; Car: Cars.

1137 **4. Validation of experimental paradigm**

1138 As visual acuity develops during the first year of life[87,88] (Supplementary **Fig S4**), one concern is that
1139 our controlled natural, gray-level stimuli may not be distinguishable to infants. Measurements of visual
1140 evoked potentials[87,88] suggest that visual acuity in 3-month-olds is around 5–8 cycles per degree (cpd)
1141 and in 6-month-olds around 10–16 cpd (Supplementary **Fig S4**). Thus, to simulate how our images may
1142 appear to infants, we filtered all images at 5 cpd. Despite being blurry, images of different categories are
1143 distinguishable and individual items retain their identity by visualization (Supplementary **Movies 1-5**).
1144

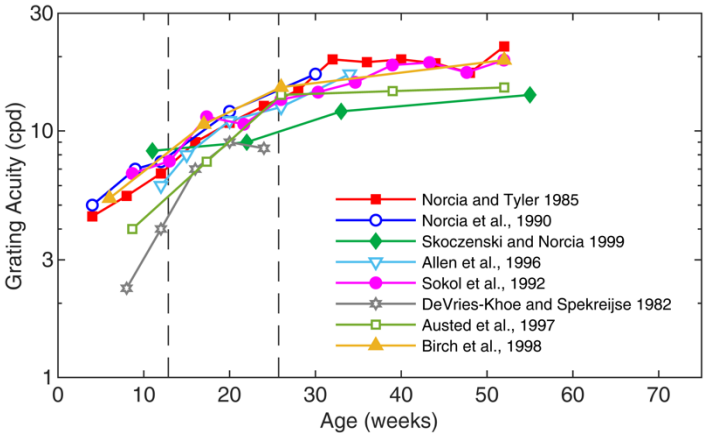

1145
1146 **Supplementary Figure 4. Grating acuity as a function of age measured with a swept spatial frequency technique**
1147 **combining EEG. (A)** Acuity growth functions are similar across studies, with acuity increasing from 5-8 cycles per
1148 degree (cpd) in 3-month-olds to around 10-16 cpd in 6-month-olds. This figure is adapted from[89].
1149
1150

5. Visual responses over occipital cortex per condition for all age groups

In the main analysis, we averaged the image-update visual responses across five conditions for each infant, as the same visual stimuli from all five stimuli categories were viewed by the infant. However, we are showing the mean Fourier amplitude spectrum over the occipital cortex for each condition for all age groups (Supplementary **Fig S5**). The response patterns across conditions at each age group is similar. To examine whether there are visual response amplitude differences between conditions by age groups, we quantified the root mean square (RMS) amplitude value of the responses at the image update frequency (4.286 Hz) and its first three harmonics (8.571 Hz, 12.857 Hz, and 17.143 Hz) for each category condition and infant. Then we used a LMM to test for an age by category interaction. The LMM was conducted over the posterior occipital ROI. Results of this analysis find no significant main effect of category ($\beta_{category}$ = 0.08, 95% CI: -0.08 – 0.24, $t_{(301)}$ = 0.97, p = .33) or category by age interaction ($\beta_{category \times age}$ = -0.04, 95% CI: -0.11 – 0.03, $t_{(301)}$ = -1.09, p = .28), which means that the visual response amplitudes are consistent across category conditions.

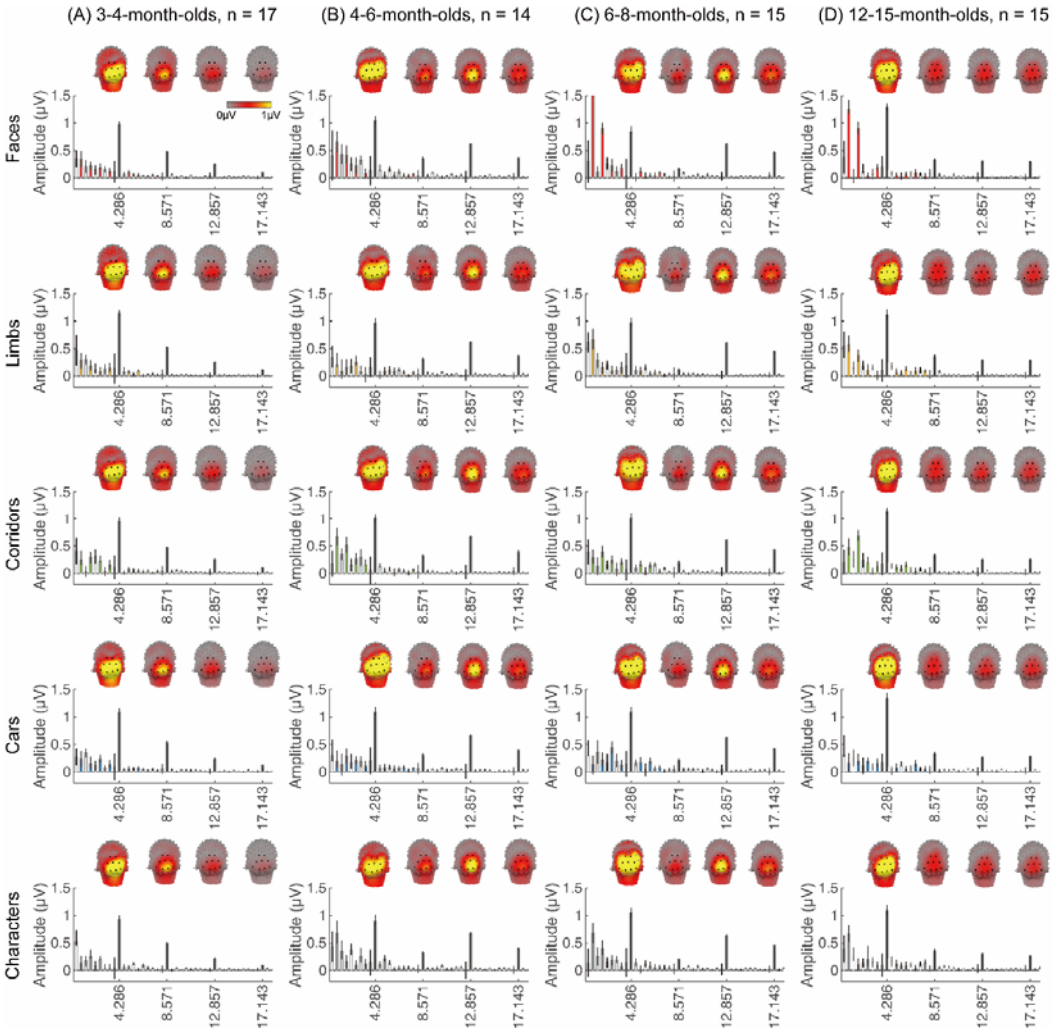

Supplementary Figure 5. Visual responses over occipital cortex at the image-update frequency and its harmonics in five category conditions in all age groups. Each column shows mean responses across infants in an age group for each condition. (A) 3-4-month-olds, n=17; (B) 4-6-month-olds, n=14; (C) 6-8-month-olds, n=15; (D) 12-15-month-olds, n=15. Graphs show the mean Fourier amplitude spectrum over the occipital ROI. The visual response is at the image update frequency (4.286 Hz) and its first three harmonics, with the mean topographies at these frequencies of interest shown on top.

6. Linear mixed model (LMM) analyses of visual responses (associated with **Figure 2**)

Supplementary Table 4: Peak latency of visual responses by age and time-window (window 1: 60-90 ms; window 2: 90-160 ms for 3-4-month-olds, and 90-110 ms for other groups)

Formula: Peak latency ~ 1 + log10(Age) × time window + (1|Participant)

Significant effects are indicated by asterisks.

Parameter	β	*CI*	*df*	*t*	*p*
Intercept	-54.61	-100.82, -8.41	118	-2.34	.021*
Age	39.77	19.51, 60.02	118	3.89	.00017***
Window	141.68	112.92, 170.45	118	9.75	7.69e-17***
Age×Window	-45.78	-58.39, -33.17	118	-7.19	6.39e-11**

Supplementary Table 5: Peak latency of visual responses by age at each of the two time-windows

Formula: Peak latency ~ 1 + log10(Age) + (1|Participant)

Significant effects are indicated by asterisks.

Window	*Parameter*	β	*CI*	*df*	*t*	*p*
Window1	Intercept	90.19	75.66, 104.72	59	12.42	4.22e-18***
	Age	-7.44	-13.82, -1.06	59	-2.33	.02*
Window2	Intercept	218.09	196.05, 240.13	59	19.80	9.64e-28***
	Age	-46.91	-56.56, -37.27	59	-9.73	7.06e-14***

Supplementary Table 6: Analysis of peak amplitude of visual responses by age and time-window

Formula: Peak amplitude ~ 1 + log10(Age) × time window + (1|Participant)

Significant effects are indicated by an asterisk.

Parameter	β	*CI*	*df*	*t*	*p*
Intercept	-18.69	-32.35, -5.03	118	-2.71	.008**
Age	3.93	-2.05, 9.92	118	1.30	.20
Window	17.24	8.66, 25.82	118	3.98	.0001***
Age×Window	-4.90	-8.66, -1.14	118	-2.58	.011*

Supplementary Table 7: Peak amplitude of visual responses by age at each of the two time-windows

Formula: Peak amplitude ~ 1 + log10(Age) + (1|Participant)

Significant effects are indicated by asterisks.

Window	*Parameter*	β	*CI*	*df*	*t*	*p*
Window1	Intercept	1.69	-3.42, 6.79	59	0.66	.51
	Age	0.91	-1.33, 3.15	59	0.82	.42
Window2	Intercept	11.16	4.80, 17.51	59	3.51	0.0009***
	Age	-3.59	-6.38, -0.81	59	-2.58	.012*

7. Frequency domain analyses of infants' categorical responses to limbs, corridors, characters and cars (associated with **Fig 3**)

Fig 3 shows the group-averaged categorical response to faces. Supplementary **Figs S6-9** show group-averaged categorical responses to the rest four conditions other than faces in four age groups. We found significant responses in 6-8-month-olds for limbs, corridors, and characters, and in 12-15 months for corridors and characters.

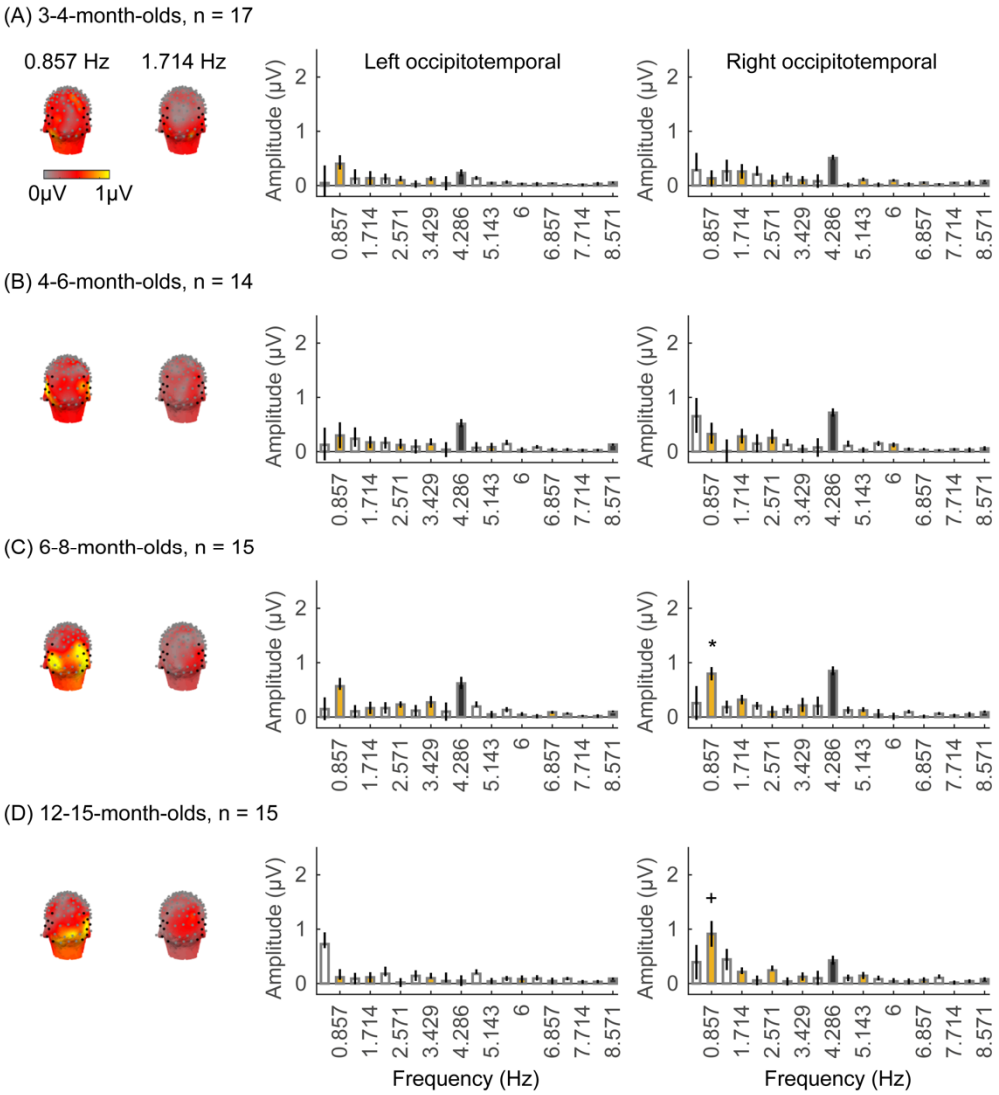

Supplementary Figure 6. Limb responses emerge over occipitotemporal electrodes after 6 months of age. Each panel shows mean responses at the category frequency (0.857 Hz) and its harmonics across infants in an age group. (A) 3-4-month-olds, n=17; (B) 4-6-month-olds; n=14; (C) 6-8-month-olds, n=15; (D) 12-15-month-olds, n=15. *Left panels in each row:* spatial distribution of categorical response at 0.857 Hz and its first harmonic. Harmonic frequencies are indicated on the top. *Right two panels in each row*: mean Fourier Amplitude Spectrum across 7 left occipitotemporal electrodes and 7 right occipitotemporal (shown in black on the left panel). Data are first averaged in each participant and then across participants. *Error bars:* standard error of the mean across participants in an age group. *Asterisk:* significant amplitude vs. zero ($p < .05$, FDR corrected). Cross: significant amplitude vs. zero ($p < .05$, with no FDR correction). *Black bars:* image frequency and harmonics; *Colored bars:* category frequency and harmonics.

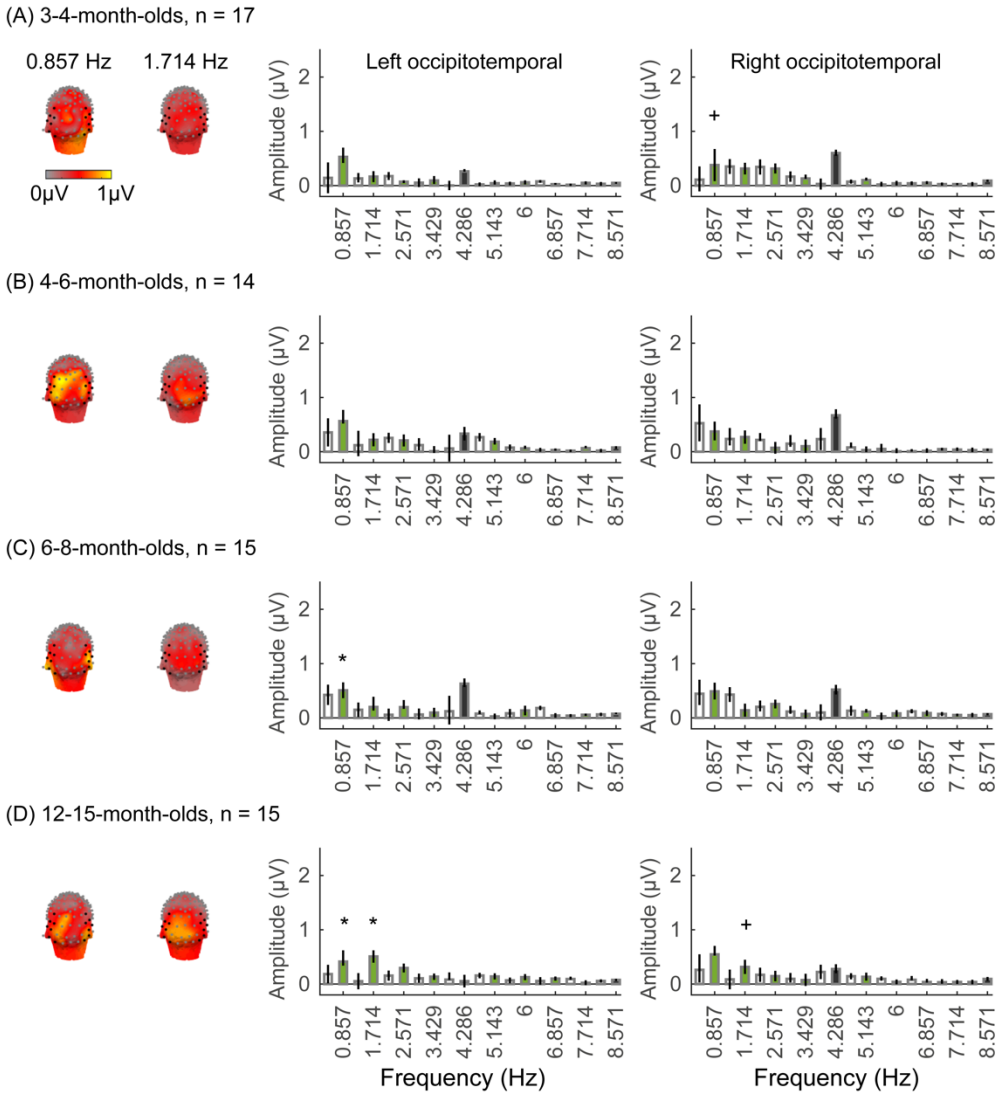

Supplementary Figure 7. Corridor responses emerge over occipitotemporal electrodes after 6 months of age. Each panel shows mean responses at the category frequency and its harmonics across infants in an age group. (A) 3-4-month-olds, n=17; (B) 4-6-month-olds; n=14; (C) 6-8-month-olds, n=15; (D) 12-15-month-olds, n=15. *Left panels in each row:* spatial distribution of categorical response at 0.857 Hz and its first harmonic. Harmonic frequencies are indicated on the top. *Right two panels in each row*: mean Fourier Amplitude Spectrum across 7 left occipitotemporal electrodes and 7 right occipitotemporal (shown in black on the left panel). Data are first averaged in each participant and then across participants. *Error bars:* standard error of the mean across participants in an age group. *Asterisks:* significant amplitude vs. zero ($p < .05$, FDR corrected). Crosses: significant amplitude vs. zero ($p < .05$, with no FDR correction). *Black bars: image frequency and harmonics; Colored bars: category frequency and harmonics.*

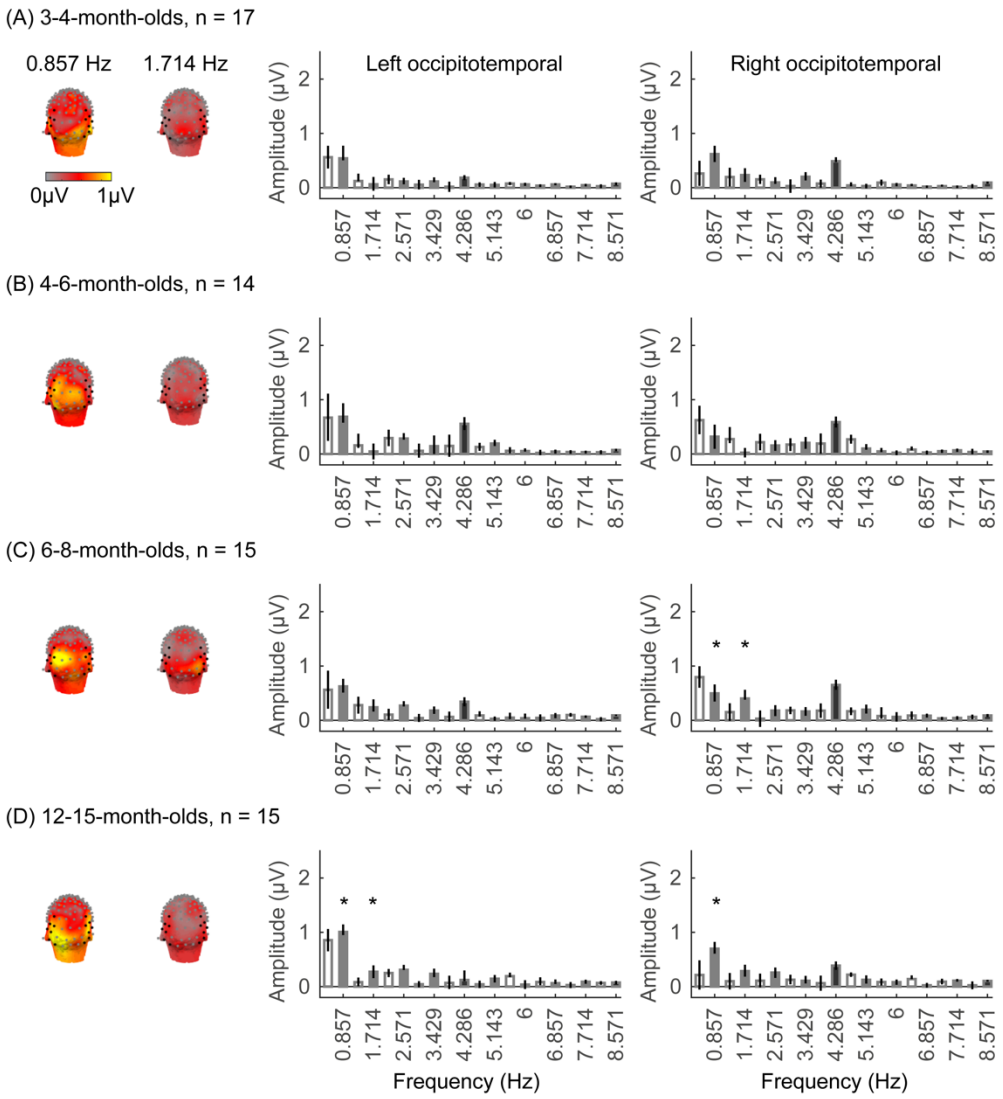

Supplementary Figure 8. Significant character responses found over occipitotemporal electrodes at 12-15 months of age. Each panel shows mean responses at the category frequency (0.857 Hz) and its harmonics across infants in an age group. (A) 3-4-month-olds, n=17; (B) 4-6-month-olds; n=14; (C) 6-8-month-olds, n=15; (D) 12-15-month-olds, n=15. *Left panels in each row:* spatial distribution of categorical response at 0.857 Hz and its first harmonic. Harmonic frequencies are indicated on the top. *Right two panels in each row*: mean Fourier Amplitude Spectrum across 7 left occipitotemporal electrodes and 7 right occipitotemporal (shown in black on the left panel). Data are first averaged in each participant and then across participants. *Error bars:* standard error of the mean across participants in an age group. *Asterisks:* significant amplitude vs. zero ($p < .05$, FDR corrected). *Black bars:* image frequency and harmonics; *Colored bars:* category frequency and harmonics.

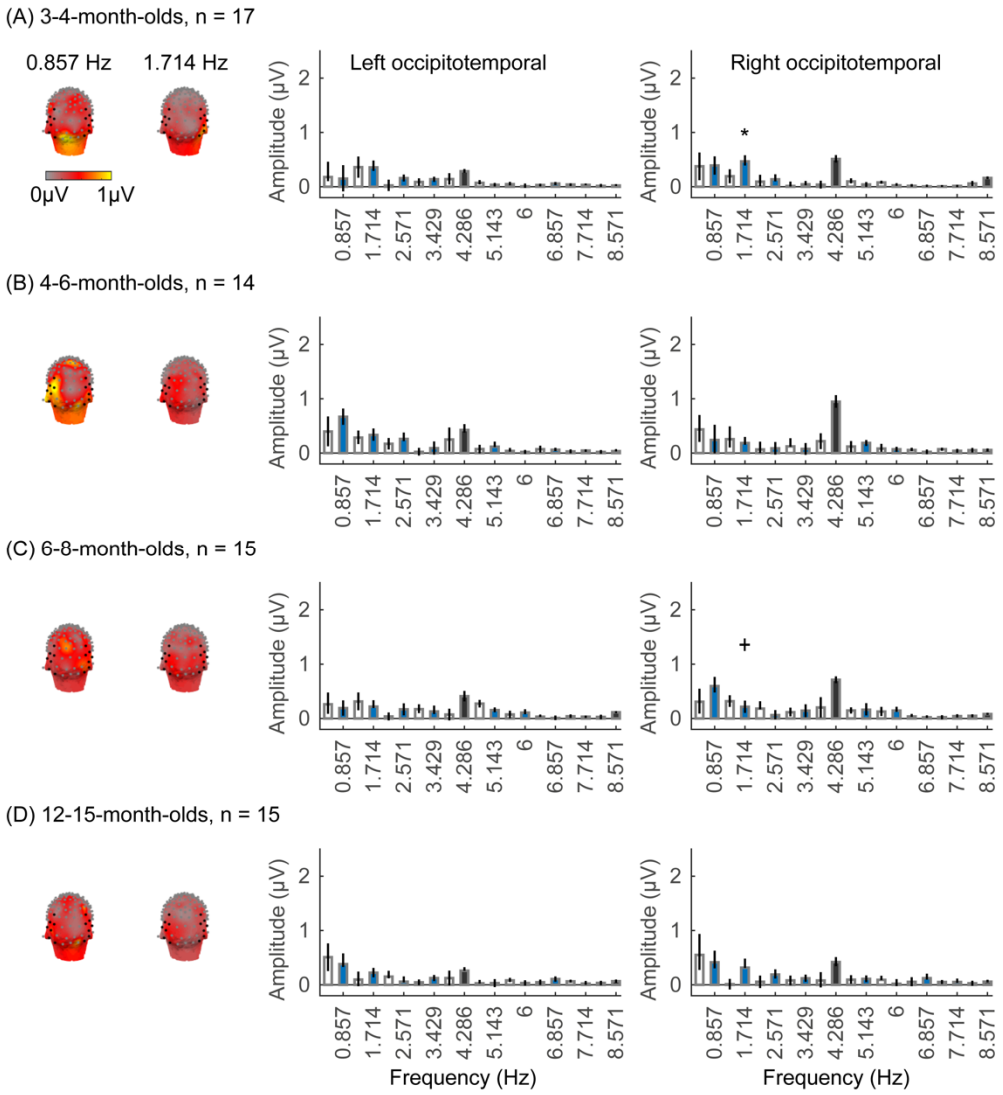

Supplementary Figure 9. Significant car responses found over occipitotemporal electrodes at 3-4 months of age. Each panel shows mean responses at the category frequency and its harmonics across infants in an age group. (A) 3-4-month-olds, n=17; (B) 4-6-month-olds; n=14; (C) 6-8-month-olds, n=15; (D) 12-15-month-olds, n=15. *Left panels in each row:* spatial distribution of categorical response at 0.857 Hz and its first harmonic. Harmonic frequencies are indicated on the top. *Right two panels in each row*: mean Fourier Amplitude Spectrum across 7 left occipitotemporal electrodes and 7 right occipitotemporal (shown in black on the left panel). Data are first averaged in each participant and then across participants. *Error bars:* standard error of the mean across participants in an age group. *Asterisk:* significant amplitude vs. zero ($p < .05$, FDR corrected). Cross: significant amplitude vs. zero ($p < .05$, with no FDR correction). *Black bars:* image frequency and harmonics; *Colored bars:* category frequency and harmonics.

8. Linear mixed model (LMM) analyses of category-selective responses.

Supplementary Table 8: Analysis of peak amplitude of waveforms of category responses by age and category.

Separate LMMs were done separately for the left occipitotemporal (OT) and right OT ROIs.

Formula: Peak amplitude ~ 1 + log10(Age) × category + (1|Participant);

Peak latency ~ 1 + log10(Age) × category + (1|Participant).

Significant effects are indicated by an asterisk.

ROI/metric	Parameter	β	CI	df	*t*	*p*
Left OT/	Intercept	-1.35	-7.36, 4.66	301	-0.44	.66
amplitude	Age	2.62	-0.02, 5.25	301	1.95	.052
	Category	0.18	-1.58, 1.93	301	0.20	.84
	Age×Category	-0.20	-0.97, 0.57	301	-0.51	.61
Left OT/	Intercept	730.29	477.96, 982.61	301	5.70	2.9e-8***
latency	Age	-97.17	-207.76, 13.43	301	-1.73	.08
	Category	-43.35	-119.43, 32.73	301	-1.12	.26
	Age×Category	20.24	-13.11, 53.58	301	1.19	.23
Right OT/	Intercept	-7.39	-14.44, -0.36	301	-2.07	.04*
amplitude	Age	5.53	2.45, 8.62	301	3.53	.0005***
	Category	2.19	0.06, 4.3	301	2.02	.04*
	Age×Category	-1.09	-2.00, -0.14	301	-2.26	.02*
Right OT/	Intercept	922.47	667.95, 1177	301	7.13	7.38e-12***
latency	Age	-173.17	-284.73, -61.61	301	-3.05	.002**
	Category	-64.41	-141.15, 12.33	301	-1.65	.10
	Age×Category	28.49	-5.15, 62.12	301	1.67	.10

Supplementary Table 9: Analysis of peak amplitude of waveforms of category responses for each category in the right OT ROI.

Formula: Peak amplitude ~ age + (1|participant)

Significant effects are indicated by an asterisk.

Category	*Parameter*	β	*CI*	*df*	*t*	*p*
Faces	Intercept	-10.43	-17.81, -3.05	59	-2.83	.006**
	Age	7.27	4.03, 10.51	59	4.50	3.30e-5***
Limbs	Intercept	2.10	-3.62, 7.83	59	0.74	.46
	Age	-2.90	-5.41, -0.38	59	-2.31	.02*
Corridors	Intercept	-4.65	-11.09, 1.81	59	-1.44	.15
	Age	0.35	-2.47, 3.18	59	0.25	.80
Characters	Intercept	-2.79	-8.06, 2.49	59	-1.06	.3
	Age	-0.66	-2.97, 1.65	59	-0.57	.57
Cars	Intercept	-4.87	-11.46, 1.73	59	-1.48	.15
	Age	0.78	-2.11, 3.67	59	0.54	.59

9. Individual level decoding analysis

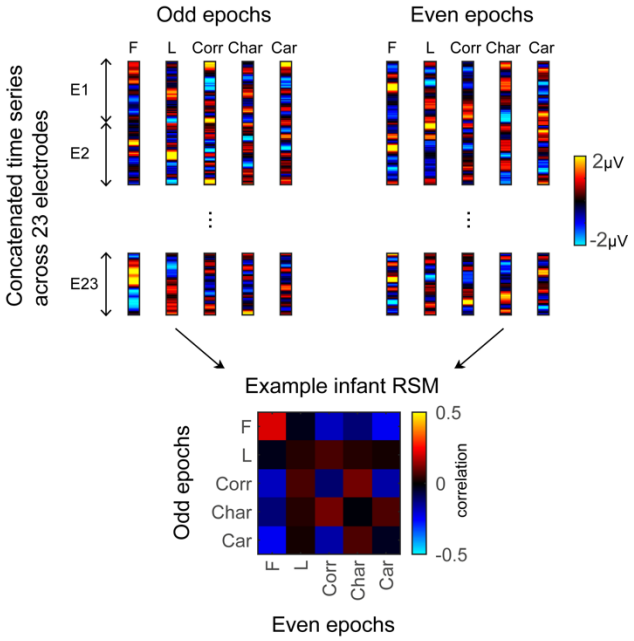

Supplementary Figure 10. Illustration of the winner-takes-all (WTA) classifier. In each individual, the time series data is split into odd and even trials. We concatenate the time series data from 23 electrodes in the left occipitotemporal, occipital, and right occipitotemporal ROIs into a pattern vector for each split half and each condition. The classifier is trained on one half of the data (i.e. odd or even trials) and tested on how well it could predict the rest half of the data (i.e. even or odd trials) for each individual. The bottom shows the representation similarity matrix (RSM) in an example infant. Each cell indicates the correlation between distributed responses to different images of the same (on diagonal) or different (off diagonal) categories. *F: Faces; L: Limbs; Corr: Corridors; Char: Characters; Car: Cars*.

Supplementary Movie 1. Movie showing gaussian lowpass filtered face stimuli shown in the experiment at 5 cycles per degree (cpd).

Supplementary Movie 2. Movie showing gaussian lowpass filtered limb stimuli shown in the experiment at 5 cycles per degree (cpd).

Supplementary Movie 3. Movie showing gaussian lowpass filtered corridor stimuli shown in the experiment at 5 cycles per degree (cpd).

Supplementary Movie 4. Movie showing gaussian lowpass filtered character stimuli shown in the experiment at 5 cycles per degree (cpd).

Supplementary Movie 5. Movie showing gaussian lowpass filtered car stimuli shown in the experiment at 5 cycles per degree (cpd).

1290 **SI References**

1291 1. Thorpe, S., Fize, D. & Marlot, C. Speed of processing in the human visual system. *Nature*
1292 **381**, 520–522 (1996).
1293 2. Grill-Spector, K. & Kanwisher, N. Visual Recognition: As Soon as You Know It Is there, You
1294 Know What It Is. *Psychological Science* **16**, (2005).
1295 3. Grill-Spector, K. & Weiner, K. S. The functional architecture of the ventral temporal cortex
1296 and its role in categorization. *Nat Rev Neurosci* **15**, 536–548 (2014).
1297 4. Bugatus, L., Weiner, K. S. & Grill-Spector, K. Task alters category representations in
1298 prefrontal but not high-level visual cortex. *Neuroimage* **155**, 437–449 (2017).
1299 5. Nordt, M. *et al.* Cortical recycling in high-level visual cortex during childhood development.
1300 *Nat Hum Behav* **5**, 1686–1697 (2021).
1301 6. Margalit, E. *et al.* Ultra-high-resolution fMRI of Human Ventral Temporal Cortex Reveals
1302 Differential Representation of Categories and Domains. *J. Neurosci.* **40**, 3008–3024 (2020).
1303 7. Gomez, J. *et al.* Microstructural proliferation in human cortex is coupled with the
1304 development of face processing. **355**, (2017).
1305 8. Stigliani, A., Weiner, K. S. & Grill-Spector, K. Temporal Processing Capacity in High-Level
1306 Visual Cortex Is Domain Specific. *Journal of Neuroscience* **35**, 12412–12424 (2015).
1307 9. Haxby, J. V. *et al.* Distributed and Overlapping Representations of Faces and Objects in
1308 Ventral Temporal Cortex. *Science* **293**, 2425–2430 (2001).
1309 10. Nordt, M. *et al.* Longitudinal development of category representations in ventral temporal
1310 cortex predicts word and face recognition. *Nat Commun* **14**, 8010 (2023).

1311 11. Kanwisher, N., McDermott, J. & Chun, M. M. The Fusiform Face Area: A Module in Human
1312 Extrastriate Cortex Specialized for Face Perception. *The Journal of Neuroscience* **17**, 4302–
1313 4311 (1997).
1314 12. Epstein, R. & Kanwisher, N. A cortical representation of the local visual environment.
1315 *Nature* **392**, 598–601 (1998).
1316 13. Downing, P. E., Jiang, Y., Shuman, M. & Kanwisher, N. A Cortical Area Selective for Visual
1317 Processing of the Human Body. *Science* **293**, 2470–2473 (2001).
1318 14. Golarai, G. *et al.* Differential development of high-level visual cortex correlates with
1319 category-specific recognition memory. *Nature Neuroscience* **10**, 512–522 (2007).
1320 15. Scherf, K. S., Behrmann, M., Humphreys, K. & Luna, B. Visual category-selectivity for faces,
1321 places and objects emerges along different developmental trajectories. *Developmental*
1322 *Science* **10**, F15–F30 (2007).
1323 16. Dehaene-Lambertz, G., Monzalvo, K. & Dehaene, S. The emergence of the visual word form:
1324 Longitudinal evolution of category-specific ventral visual areas during reading acquisition.
1325 *PLOS Biology* **16**, e2004103 (2018).
1326 17. Spriet, C., Abassi, E., Hochmann, J.-R. & Papeo, L. Visual object categorization in infancy.
1327 *Proc. Natl. Acad. Sci. U.S.A.* **119**, e2105866119 (2022).
1328 18. Mondloch, C. J. *et al.* Face Perception During Early Infancy. *Psychol Sci* **10**, 419–422 (1999).
1329 19. Quinn, P. C., Eimas, P. D. & Rosenkrantz, S. L. Evidence for Representations of Perceptually
1330 Similar Natural Categories by 3-Month-Old and 4-Month-Old Infants. *Perception* **22**, 463–
1331 475 (1993).

1332 20. Younger, B. A. & Fearing, D. D. Parsing Items into Separate Categories: Developmental
1333 Change in Infant Categorization. *Child Development* **70**, 291–303 (1999).
1334 21. Conte, S., Richards, J. E., Guy, M. W., Xie, W. & Roberts, J. E. Face-sensitive brain responses
1335 in the first year of life. *NeuroImage* **211**, 116602 (2020).
1336 22. Farzin, F., Hou, C. & Norcia, A. M. Piecing it together: Infants' neural responses to face and
1337 object structure. *Journal of Vision* **12**, 6 (2012).
1338 23. de Heering, A. & Rossion, B. Rapid categorization of natural face images in the infant right
1339 hemisphere. *eLife* **4**, e06564 (2015).
1340 24. Bayet, L. *et al.* Temporal dynamics of visual representations in the infant brain.
1341 *Developmental Cognitive Neuroscience* **45**, 100860 (2020).
1342 25. Xie, S. *et al.* Visual category representations in the infant brain. *Current Biology* **32**, 5422-
1343 5432.e6 (2022).
1344 26. Deen, B. *et al.* Organization of high-level visual cortex in human infants. *Nat Commun* **8**,
1345 13995 (2017).
1346 27. Kosakowski, H. L. *et al.* Selective responses to faces, scenes, and bodies in the ventral visual
1347 pathway of infants. *Current Biology* **32**, 265-274.e5 (2022).
1348 28. Kanwisher, N. Functional specificity in the human brain: A window into the functional
1349 architecture of the mind. *Proceedings of the National Academy of Sciences* **107**, 11163–
1350 11170 (2010).
1351 29. Sugita, Y. Innate face processing. *Current Opinion in Neurobiology* **19**, 39–44 (2009).
1352 30. Mahon, B. Z. & Caramazza, A. What drives the organization of object knowledge in the
1353 brain? *Trends in Cognitive Sciences* **15**, 97–103 (2011).

1354 31. Bi, Y., Wang, X. & Caramazza, A. Object Domain and Modality in the Ventral Visual Pathway.
1355 *Trends in Cognitive Sciences* **20**, 282–290 (2016).
1356 32. Behrmann, M. & Plaut, D. C. A vision of graded hemispheric specialization. *Ann N Y Acad Sci*
1357 **1359**, 30–46 (2015).
1358 33. Pascalis, O., de Schonen, S., Morton, J., Deruelle, C. & Fabre-Grenet, M. Mother's face
1359 recognition by neonates: A replication and an extension. *Infant Behavior & Development*
1360 **18**, 79–85 (1995).
1361 34. Johnson, M. H., Dziurawiec, S., Ellis, H. & Morton, J. Newborns' preferential tracking of face-
1362 like stimuli and its subsequent decline. *Cognition* **40**, 1–19 (1991).
1363 35. Buiatti, M. *et al.* Cortical route for facelike pattern processing in human newborns.
1364 *Proceedings of the National Academy of Sciences* **116**, 4625–4630 (2019).
1365 36. Dehaene, S. *et al.* How Learning to Read Changes the Cortical Networks for Vision and
1366 Language. *Science* **330**, 1359–1364 (2010).
1367 37. Arcaro, M. J., Schade, P. F. & Livingstone, M. S. Universal Mechanisms and the Development
1368 of the Face Network: What You See Is What You Get. *Annu Rev Vis Sci* **5**, 341–372 (2019).
1369 38. Scott, L. S. & Arcaro, M. J. A domain-relevant framework for the development of face
1370 processing. *Nat Rev Psychol* **2**, 183–195 (2023).
1371 39. Livingstone, M. S. *et al.* Development of the macaque face-patch system. *Nat Commun* **8**,
1372 14897 (2017).
1373 40. Arcaro, M. J., Schade, P. F., Vincent, J. L., Ponce, C. R. & Livingstone, M. S. Seeing faces is
1374 necessary for face-domain formation. *Nat Neurosci* **20**, 1404–1412 (2017).

1375 41. Fausey, C. M., Jayaraman, S. & Smith, L. B. From faces to hands: Changing visual input in the
1376 first two years. *Cognition* **152**, 101–107 (2016).
1377 42. Jayaraman, S., Fausey, C. M. & Smith, L. B. Why are faces denser in the visual experiences of
1378 younger than older infants? *Developmental Psychology* **53**, 38–49 (2017).
1379 43. Allen, E. J. *et al.* A massive 7T fMRI dataset to bridge cognitive neuroscience and artificial
1380 intelligence. *Nat Neurosci* **25**, 116–126 (2022).
1381 44. Lerma-Usabiaga, G., Carreiras, M. & Paz-Alonso, P. M. Converging evidence for functional
1382 and structural segregation within the left ventral occipitotemporal cortex in reading.
1383 *Proceedings of the National Academy of Sciences* **115**, E9981–E9990 (2018).
1384 45. Jagadeesh, A. V. & Gardner, J. L. Texture-like representation of objects in human visual
1385 cortex. *Proceedings of the National Academy of Sciences* **119**, e2115302119 (2022).
1386 46. Farzin, F., Hou, C. & Norcia, A. M. Piecing it together: Infants' neural responses to face and
1387 object structure. *Journal of Vision* **12**, 6 (2012).
1388 47. Heinrich, S. P., Mell, D. & Bach, M. Frequency-domain analysis of fast oddball responses to
1389 visual stimuli: A feasibility study. *International Journal of Psychophysiology* **73**, 287–293
1390 (2009).
1391 48. Liu-Shuang, J., Norcia, A. M. & Rossion, B. An objective index of individual face
1392 discrimination in the right occipito-temporal cortex by means of fast periodic oddball
1393 stimulation. *Neuropsychologia* **52**, 57–72 (2014).
1394 49. Rekow, D. *et al.* Odor-driven face-like categorization in the human infant brain. *Proceedings*
1395 *of the National Academy of Sciences* **118**, e2014979118 (2021).

1396 50. Taylor, M. J., McCarthy, G., Saliba, E. & Degiovanni, E. ERP evidence of developmental
1397 changes in processing of faces. *Clinical Neurophysiology* **110**, 910–915 (1999).
1398 51. Xie, W., McCormick, S. A., Westerlund, A., Bowman, L. C. & Nelson, C. A. Neural Correlates
1399 of Facial Emotion Processing in Infancy. *Dev Sci* **22**, e12758 (2019).
1400 52. Gentile, F. & Rossion, B. Temporal frequency tuning of cortical face-sensitive areas for
1401 individual face perception. *NeuroImage* **90**, 256–265 (2014).
1402 53. Retter, T. L., Jiang, F., Webster, M. A. & Rossion, B. All-or-none face categorization in the
1403 human brain. *NeuroImage* **213**, 116685 (2020).
1404 54. Peykarjou, S. Frequency tagging with infants: The visual oddball paradigm. *Front. Psychol.*
1405 **13**, 1015611 (2022).
1406 55. Guy, M. W., Zieber, N. & Richards, J. E. The Cortical Development of Specialized Face
1407 Processing in Infancy. *Child Dev* **87**, 1581–1600 (2016).
1408 56. Halit, H., Csibra, G., Volein, Á. & Johnson, M. H. Face-sensitive cortical processing in early
1409 infancy. *Journal of Child Psychology and Psychiatry* **45**, 1228–1234 (2004).
1410 57. Goren, C. C., Sarty, M. & Wu, P. Y. Visual following and pattern discrimination of face-like
1411 stimuli by newborn infants. *Pediatrics* **56**, 544–549 (1975).
1412 58. Halit, H., de Haan, M. & Johnson, M. H. Cortical specialisation for face processing: face-
1413 sensitive event-related potential components in 3- and 12-month-old infants. *NeuroImage*
1414 **19**, 1180–1193 (2003).
1415 59. Macchi Cassia, V., Kuefner, D., Westerlund, A. & Nelson, C. A. A behavioural and ERP
1416 investigation of 3-month-olds' face preferences. *Neuropsychologia* **44**, 2113–2125 (2006).

1417 60. Tzourio-Mazoyer, N. *et al.* Neural Correlates of Woman Face Processing by 2-Month-Old
1418 Infants. *NeuroImage* **15**, 454–461 (2002).
1419 61. Rossion, B. Biomarkers of Face Perception in Autism Spectrum Disorder: Time to Shift to
1420 Fast Periodic Visual Stimulation With Electroencephalography? *Biological Psychiatry:*
1421 *Cognitive Neuroscience and Neuroimaging* **5**, 258–260 (2020).
1422 62. Vettori, S. *et al.* Reduced neural sensitivity to rapid individual face discrimination in autism
1423 spectrum disorder. *NeuroImage: Clinical* **21**, 101613 (2019).
1424 63. Farran, E. K. *et al.* Characterizing the neural signature of face processing in Williams
1425 syndrome via multivariate pattern analysis and event related potentials. *Neuropsychologia*
1426 **142**, 107440 (2020).
1427 64. Kobayashi, M., Kakigi, R., Kanazawa, S. & Yamaguchi, M. K. Infants' recognition of their
1428 mothers' faces in facial drawings. *Dev Psychobiol* **62**, 1011–1020 (2020).
1429 65. Peelen, M. V., Fei-Fei, L. & Kastner, S. Neural mechanisms of rapid natural scene
1430 categorization in human visual cortex. *Nature* **460**, 94–97 (2009).
1431 66. Cantlon, J. F., Pinel, P., Dehaene, S. & Pelphrey, K. A. Cortical Representations of Symbols,
1432 Objects, and Faces Are Pruned Back during Early Childhood. *Cerebral Cortex* **21**, 191–199
1433 (2011).
1434 67. Cohen, M. A. *et al.* Representational similarity precedes category selectivity in the
1435 developing ventral visual pathway. *NeuroImage* **197**, 565–574 (2019).
1436 68. Grotheer, M. *et al.* White matter myelination during early infancy is linked to spatial
1437 gradients and myelin content at birth. *Nat Commun* **13**, 997 (2022).

1438 69. Natu, V. S. *et al.* Infants' cortex undergoes microstructural growth coupled with myelination
1439 during development. *Commun Biol* **4**, 1191 (2021).
1440 70. Tooley, U. A., Bassett, D. S. & Mackey, A. P. Environmental influences on the pace of brain
1441 development. *Nat Rev Neurosci* **22**, 372–384 (2021).
1442 71. Adibpour, P. *et al.* Characterizing the temporal dynamics and maturation of resting-state
1443 activity: an EEG microstate study in preterm and full-term infants. 2024.03.19.585608
1444 Preprint at https://doi.org/10.1101/2024.03.19.585608 (2024).
1445 72. Lebenberg, J. *et al.* Mapping the asynchrony of cortical maturation in the infant brain: A
1446 MRI multi-parametric clustering approach. *NeuroImage* **185**, 641–653 (2019).
1447 73. Gilmore, J. H., Knickmeyer, R. C. & Gao, W. Imaging structural and functional brain
1448 development in early childhood. *Nat Rev Neurosci* **19**, 123–137 (2018).
1449 74. Bannert, M. M. & Bartels, A. Visual cortex: Big data analysis uncovers food specificity.
1450 *Current Biology* **32**, R1012–R1015 (2022).
1451 75. Jain, N. Selectivity for food in human ventral visual cortex. *Communications Biology* **6**, 175
1452 (2023).
1453 76. Pennock, I. M. L. *et al.* Color-biased regions in the ventral visual pathway are food selective.
1454 *Current Biology* **33**, 134-146.e4 (2023).
1455 77. Willenbockel, V. *et al.* Controlling low-level image properties: The SHINE toolbox. *Behavior*
1456 *Research Methods* **42**, 671–684 (2010).
1457 78. Norcia, A. M., Pei, F. & Kohler, P. J. Evidence for long-range spatiotemporal interactions in
1458 infant and adult visual cortex. *Journal of Vision* **17**, 12 (2017).

79. Kohler, P. J., Barzegaran, E., Norcia, A. M. & McCandliss, B. D. Parietal Contributions to Abstract Numerosity Measured with Steady State Visual Evoked Potentials. 2020.08.06.239889 Preprint at https://doi.org/10.1101/2020.08.06.239889 (2020).

80. Victor, J. D. & Mast, J. A new statistic for steady-state evoked potentials. *Electroencephalography and Clinical Neurophysiology* **78**, 378–388 (1991).

81. Appelbaum, L. G., Wade, A. R., Vildavski, V. Y., Pettet, M. W. & Norcia, A. M. Cue-Invariant Networks for Figure and Background Processing in Human Visual Cortex. *J. Neurosci.* **26**, 11695–11708 (2006).

82. Blair, R. C. & Karniski, W. An alternative method for significance testing of waveform difference potentials. *Psychophysiology* **30**, 518–524 (1993).

83. Maris, E. & Oostenveld, R. Nonparametric statistical testing of EEG- and MEG-data. *Journal of Neuroscience Methods* **164**, 177–190 (2007).

84. Bosker, R. & Snijders, T. Multilevel Analysis: An Introduction to Basic and Advanced Multilevel Modeling. 1–368 (2011).

85. Li, G. *et al.* Mapping longitudinal development of local cortical gyrification in infants from birth to 2 years of age. *J Neurosci* **34**, 4228–4238 (2014).

86. Grieve, P. G., Emerson, R. G., Fifer, W. P., Isler, J. R. & Stark, R. I. Spatial correlation of the infant and adult electroencephalogram. *Clinical Neurophysiology* **114**, 1594–1608 (2003).

87. Norcia, A. M. & Tyler, C. W. Spatial frequency sweep VEP: Visual acuity during the first year of life. *Vision Research* **25**, 1399–1408 (1985).

88. Norcia, A. M., Tyler, C. W. & Hamer, R. D. Development of contrast sensitivity in the human infant. *Vision Research* **30**, 1475–1486 (1990).

1481 89. Norcia, A. M. Development of vision in infancy. in *Adler's Physiology of the Eye* 531–551
1482 (Elsevier Health Sciences, 2011).
1483